peroxide into water to prevent production of hydroxyl radicals. Because reduction of GPx and catalase activities could induce accumulation of hydrogen peroxide, we measured the GPx and catalase activities after mProx24 cells had been treated with albumin for 10 min. Figure 8B showed that both enzymatic activities were reduced by albumin. These results indicate that changes in GPx and catalase activities could be responsible for the accumulation of intracellular ROS after exposure of mProx24 cells to albumin.

Measurement of the Total Reduced Form of Glutathione

Generally, intracellular proteins do not contain disulfide bonds because the high cytosolic concentration of free sulfhydryl (-SH) reducing agents breaks such bonds (42). We hypothesized that a large amount of proteins with disulfide bonds, such as albumin and apoTf, might lead to oxidative stress when ingested into cells. To address this, we measured the shift in intracellular GSH levels. GSH is a naturally occurring tripeptide whose nucleophilic and reducing properties play a central role in the antioxidant system of most aerobic cells. GSH is crucial to the maintenance of the -SH level of proteins in cells (43). Hence, we determined the quantity of the total reduced form of GSH under various conditions of albumin loading. The quantity of GSH increased after albumin starvation, but did not show any marked change compared with control cells after treatment with albumin for 10 min (Figure 8C). Our findings suggest that the increase in GSH was induced by long-term upregulation of intracellular ROS, and that GSH was not consumed for at least 10 min after the cells were exposed to albumin.

Discussion

We have previously constructed gene expression profiles by means of direct sequencing procedures (26,29), and identified several immunity-related genes, such as MHC class I and II, by comparing the profiles of control and disease model proximal tubular cells. Renal MHC proteins are expressed in response to inflammation and renal injury, and their expression is thought to be regulated solely by IFN-γ (44). Because the IFN-γ pathway usually requires the activation of Stat1 (45,46), we hypothesized that proteinuria could activate proximal tubular cells directly by activation of the STAT signaling pathway. Our results indicate that albumin activates proximal tubular cells in an IFN-γ–independent manner after ROS-mediated STAT activation.

Our data also demonstrate that Stat1/5 and Stat3 show different responses to albumin. The activation of Stat1 and Stat5 was clearly identified within 15 min. In contrast, no manifest activation of Stat3 could be identified after a 1-h exposure to albumin, and activation of Stat3 was observed only after a 4-h exposure. The mechanisms responsible for these different responses are still obscure, but the differences may depend on the cell type. In macrophages, Stat1 has been reported to induce sterilizing activity and the production of various complements, chemokines, and adhesion molecules (3). Stat5, which was originally identified as a mammary gland factor regulated by prolactin, is also activated by multiple cytokines, including IL-2, IL-3, and GM-CSF, which are macrophage-activating factors. In contrast, IL-10–induced Stat3 activation suppresses macrophage activity, and mice lacking Stat3 show abnormally enhanced macrophage activity and develop chronic inflammation (47). The different responses of Stat1/5 and Stat3 in the renal proximal tubular cell line seem to be similar to those in macrophages, suggesting that albumin overloading can induce proinflammatory processes. Stat3 is activated by various cytokines, such as IL-6, that are also induced by IFN-γ (30). Therefore, the activation of Stat3 at a late stage after albumin overloading might be due to a secondary response after Stat1 activation by albumin.

ROS generation was even observed in the control mProx24 cells after starvation, leading to a slight activation of Stat1 and Stat5. This is a previously reported result that supports our finding that serum deprivation can induce elevated ROS and an oxidative state in cells (48). Nuclear factor kappa B (NF-κB) is also induced by ROS (38) and is one of the key components that cause immune reactions in kidneys (49). A recent report of a new and interesting Stat5 signal transduction mechanism suggests that Stat5 could be a potential activator of NF-κB in some types of hematopoietic cells (50). In addition, many IFN-γ–inducible genes, such as RANTES and MCP-1, were found to be induced synergistically by IFN-γ and TNF-α (51). This synergism is reportedly involved in the interaction between activated Stat1 and NF-κB (11,30). Hence, the activation of Stat1 and Stat5 by albumin may be important in the induction of transcripts that cause kidney disease progression.

Recent reports have demonstrated rapid and significant increases in intracellular ROS after growth factor or cytokine stimulation. These types of ROS appear to be essential for a host of downstream signaling events, including cell proliferation, apoptosis, and inflammation, and thus contribute to the development of diseases (52). Simon *et al.* (7) reported that members of the STAT family of transcription factors were activated in fibroblasts and A-431 carcinoma cells in response to H_2O_2. This activation occurred within 5 min, could be inhibited by antioxidants, and did not require protein synthesis. These findings hence indicate that the JAK/STAT pathway responds to intracellular ROS.

Our results indicate that the membrane-bound NADPH oxidase system seems to be relevant in the induction of ROS by albumin. It has been found that the activity of a membrane-bound NADPH oxidase often mediates intracellular generation of ROS in response to ligands (40,41). The ROS in macrophages are also produced by NADPH oxidase after phagocytosis (53). Hence, it is particularly interesting that the endocytic uptake of albumin in renal proximal tubular cells seems also to be responsible for ROS generation. Further investigation is needed, however, to clarify the precise mechanisms of ROS generation by NADPH oxidase after albumin overloading. Our results also indicate that the GPx and catalase activities changed within 10 min after albumin loading, suggesting that albumin could interfere with GPx and catalase activities by way of glia maturation factor–beta (54). The low activities of GPx and catalase could be responsible for the accumulation of the intracellular ROS after albumin ingestion into mProx24 cells. Hence, it seems that not only the ROS generating system but also the ROS-scavenging system may contribute to the induction of ROS by albumin.

We next focus on the amino acid sequences of albumin and apoTf. The amino acid sequences of human, bovine, and rodent albumin are highly homologous. Albumin itself contains a high percentage of cysteine that is organized into a characteristic repeating disulfide pattern (55). Generally, intracellular proteins do not contain disulfide bonds because the high cytosolic concentration of free sulfhydryl (−SH) reducing agents breaks such bonds (42). We hypothesized that a large amount of proteins with disulfide bonds, such as albumin and apoTf, might cause oxidative stress when ingested into the cells. However, our data indicate that the amount of GSH was not changed for at least 10 min after albumin overloading, suggesting that disulfide bonds are not a primary cause of ROS induction.

Several mechanisms have been proposed by which ROS might activate intracellular kinases such as Jak2. One of these mechanisms is inactivation of protein tyrosine phosphatases (PTPs) that may be susceptible to oxidation (56). Tyrosine phosphorylation of proteins is dependent on the balance between kinases and PTPs within a cell. Therefore, it is feasible that inactivation of PTPs could induce tyrosine phosphorylation of Jak2. Another possible mechanism involves Fyn, a member of the *src* family, which can regulate the activation of Jak2 by H_2O_2 in fibroblasts (57). These proposed mechanisms need to be verified in future studies.

The fact that almost all cytokines activate the JAK/STAT pathway suggests that STATs play important roles in the inflammatory process. Our results suggest that albumin, a major component of proteinuria, exerts cytokine-like effects to activate proximal tubular cells after ROS-mediated STAT activation. The activated STAT signaling could then result in cell proliferation, production of several cytokines/growth factors, and induction of immune responses that are presumably involved in the progression of kidney diseases. The results reported here could thus provide an insight into the intrinsic toxicity of proteinuria and may provide further clues regarding therapeutic approaches to inhibition of the signal transduction pathways involved in proteinuria.

Acknowledgments

This study was supported in part by a Grant-in-Aid for Scientific Research from the Ministry of Education, Science, Sports and Culture, Japan, and in part by Renal Discoveries, the Baxter Extramural Grant Program, USA. We thank Dr. Toshio Hirano (Department of Molecular Oncology, Graduate School of Medicine, Osaka University) for his valuable suggestion about STAT signaling pathways and Naoko Horimoto for her technical assistance.

References

1. Farrar MA, Schreiber RD: The molecular cell biology of interferon-gamma and its receptor. *Annu Rev Immunol* 11: 571–611, 1993
2. Darnell JE Jr, Kerr IM, Stark GR: Jak-STAT pathways and transcriptional activation in response to IFNs and other extracellular signaling proteins. *Science* 264: 1415–1421, 1994
3. Bach EA, Aguet M, Schreiber RD: The IFN gamma receptor: A paradigm for cytokine receptor signaling. *Annu Rev Immunol* 15: 563–591, 1997
4. Darnell JE Jr: STATs and gene regulation. *Science* 277: 1630–1635, 1997
5. Ihle JN: The Stat family in cytokine signaling. *Curr Opin Cell Biol* 13: 211–217, 2001
6. Herrington J, Smit LS, Schwartz J, Carter-Su C: The role of STAT proteins in growth hormone signaling. *Oncogene* 19: 2585–2597, 2000
7. Simon AR, Rai U, Fanburg BL, Cochran BH: Activation of the JAK-STAT pathway by reactive oxygen species. *Am J Physiol* 275: C1640–1652, 1998
8. Akira S: Roles of STAT3 defined by tissue-specific gene targeting. *Oncogene* 19: 2607–2611, 2000
9. Levy DE: Physiological significance of STAT proteins: Investigations through gene disruption in vivo. *Cell Mol Life Sci* 55: 1559–1567, 1999
10. Ihle JN: Cytokine receptor signalling. *Nature* 377: 591–594, 1995
11. Ramana CV, Chatterjee-Kishore M, Nguyen H, Stark GR: Complex roles of Stat1 in regulating gene expression. *Oncogene* 19: 2619–2627, 2000
12. Lin JX, Leonard WJ: The role of Stat5a and Stat5b in signaling by IL-2 family cytokines. *Oncogene* 19: 2566–2576, 2000
13. Hirano T, Ishihara K, Hibi M: Roles of STAT3 in mediating the cell growth, differentiation and survival signals relayed through the IL-6 family of cytokine receptors. *Oncogene* 19: 2548–2556, 2000
14. Mui AL: The role of STATs in proliferation, differentiation, and apoptosis. *Cell Mol Life Sci* 55: 1547–1558, 1999
15. Buettner R, Mora LB, Jove R: Activated STAT signaling in human tumors provides novel molecular targets for therapeutic intervention. *Clin Cancer Res* 8: 945–954, 2002
16. Benigni A, Remuzzi G: How renal cytokines and growth factors contribute to renal disease progression. *Am J Kidney Dis* 37: S21–24, 2001
17. Deckers JG, Van Der Woude FJ, Van Der Kooij SW, Daha MR: Synergistic effect of IL-1alpha, IFN-gamma, and TNF-alpha on RANTES production by human renal tubular epithelial cells in vitro. *J Am Soc Nephrol* 9: 194–202, 1998
18. Ruggenenti P, Perna A, Mosconi L, Pisoni R, Remuzzi G: Urinary protein excretion rate is the best independent predictor of ESRF in non-diabetic proteinuric chronic nephropathies. "Gruppo Italiano di Studi Epidemiologici in Nefrologia" (GISEN). *Kidney Int* 53: 1209–1216, 1998
19. Peterson JC, Adler S, Burkart JM, Greene T, Hebert LA, Hunsicker LG, King AJ, Klahr S, Massry SG, Seifter JL: Blood pressure control, proteinuria, and the progression of renal disease. The Modification of Diet in Renal Disease Study. *Ann Intern Med* 123: 754–762, 1995
20. Mogensen CE: Microalbuminuria predicts clinical proteinuria and early mortality in maturity-onset diabetes. *N Engl J Med* 310: 356–360, 1984
21. Viberti GC, Hill RD, Jarrett RJ, Argyropoulos A, Mahmud U, Keen H: Microalbuminuria as a predictor of clinical nephropathy in insulin-dependent diabetes mellitus. *Lancet* 8287: 1430–1432, 1982
22. Pinto-Sietsma SJ, Janssen WM, Hillege HL, Navis G, De Zeeuw D, De Jong PE: Urinary albumin excretion is associated with renal functional abnormalities in a nondiabetic population. *J Am Soc Nephrol* 11: 1882–1888, 2000
23. Remuzzi G: Abnormal protein traffic through the glomerular barrier induces proximal tubular cell dysfunction and causes renal injury. *Curr Opin Nephrol Hypertens* 4: 339–342, 1995
24. Okubo K, Hori N, Matoba R, Niiyama T, Matsubara K: A novel system for large-scale sequencing of cDNA by PCR amplification. *DNA Seq* 2: 137–144, 1991
25. Okubo K, Hori N, Matoba R, Niiyama T, Fukushima A, Kojima Y, Matsubara K: Large scale cDNA sequencing for analysis of

quantitative and qualitative aspects of gene expression. *Nat Genet* 2: 173–179, 1992
26. Nakajima H, Takenaka M, Kaimori JY, Nagasawa Y, Kosugi A, Kawamoto S, Imai E, Hori M, Okubo K: Gene expression profile of renal proximal tubules regulated by proteinuria. *Kidney Int* 61: 1577–1587, 2002
27. Takenaka M, Imai E, Nagasawa Y, Matsuoka Y, Moriyama T, Kaneko T, Hori M, Kawamoto S, Okubo K: Gene expression profiles of the collecting duct in the mouse renal inner medulla. *Kidney Int* 57: 19–24, 2000
28. Takenaka M, Imai E: Functional genomics in nephrology. *Nephrol Dial Transplant* 14: 1–3, 1999
29. Takenaka M, Imai E, Kaneko T, Ito T, Moriyama T, Yamauchi A, Hori M, Kawamoto S, Okubo K: Isolation of genes identified in mouse renal proximal tubule by comparing different gene expression profiles. *Kidney Int* 53: 562–572, 1998
30. Boehm U, Klamp T, Groot M, Howard JC: Cellular responses to interferon-gamma. *Annu Rev Immunol* 15: 749–795, 1997
31. Zoja C, Benigni A, Remuzzi G: Protein overload activates proximal tubular cells to release vasoactive and inflammatory mediators. *Exp Nephrol* 7: 420–428, 1999
32. Banu N, Meyers CM: IFN-gamma and LPS differentially modulate class II MHC and B7-1 expression on murine renal tubular epithelial cells. *Kidney Int* 55: 2250–2263, 1999
33. Takaya K, Koya D, Isono M, Sugimoto T, Sugaya T, Kashiwagi A, Haneda M: Involvement of ERK pathway in albumin-induced MCP-1 expression in mouse proximal tubular cells. *Am J Physiol Renal Physiol* 284: F1037–F1045, 2003
34. Kamijo A, Kimura K, Sugaya T, Yamanouchi M, Hase H, Kaneko T, Hirata Y, Goto A, Fujita T, Omata M: Urinary free fatty acids bound to albumin aggravate tubulointerstitial damage. *Kidney Int* 62: 1628–1637, 2002
35. Kisseleva T, Bhattacharya S, Braunstein J, Schindler CW: Signaling through the JAK/STAT pathway, recent advances and future challenges. *Gene* 285: 1–24, 2002
36. Bolen JB, Brugge JS: Leukocyte protein tyrosine kinases: Potential targets for drug discovery. *Annu Rev Immunol* 15: 371–404, 1997
37. Tang S, Leung JC, Abe K, Chan KW, Chan LY, Chan TM, Lai KN: Albumin stimulates interleukin-8 expression in proximal tubular epithelial cells in vitro and in vivo. *J Clin Invest* 111: 515–527, 2003
38. Morigi M, Macconi D, Zoja C, Donadelli R, Buelli S, Zanchi C, Ghilardi M, Remuzzi G: Protein overload-induced NF-kappaB activation in proximal tubular cells requires H(2)O(2) through a PKC-dependent pathway. *J Am Soc Nephrol* 13: 1179–1189, 2002
39. Curtin JF, Donovan M, Cotter TG: Regulation and measurement of oxidative stress in apoptosis. *J Immunol Methods* 265: 49–72, 2002
40. Thannickal VJ, Hassoun PM, White AC, Fanburg BL: Enhanced rate of H_2O_2 release from bovine pulmonary artery endothelial cells induced by TGF-beta 1. *Am J Physiol* 265: L622–L626, 1993
41. Irani K, Xia Y, Zweier JL, Sollott SJ, Der CJ, Fearon ER, Sundaresan M, Finkel T, Goldschmidt-Clermont PJ: Mitogenic signaling mediated by oxidants in Ras-transformed fibroblasts. *Science* 275: 1649–1652, 1997
42. Alberts B, Bray D, Lewis J, Raff M, Roberts K, Watson JD: *Molecular Biology of the Cell*, 2nd ed., New York, Garland, 1989
43. Dolphin D, Poulson R, Avramovic O: *Glutathione: Chemical, Biochemical and Medical Aspects*, Vols. A and B, New York, J. Wiley, 1989
44. Takei Y, Sims TN, Urmson J, Halloran PF: Central role for interferon-gamma receptor in the regulation of renal MHC expression. *J Am Soc Nephrol* 11: 250–261, 2000
45. Durbin JE, Hackenmiller R, Simon MC, Levy DE: Targeted disruption of the mouse *Stat1* gene results in compromised innate immunity to viral disease. PG-443-50. *Cell* 84: 443–450, 1996
46. Meraz MA, White JM, Sheehan KC, Bach EA, Rodig SJ, Dighe AS, Kaplan DH, Riley JK, Greenlund AC, Campbell D, Carver-Moore K, DuBois RN, Clark R, Aguet M, Schreiber RD: Targeted disruption of the Stat1 gene in mice reveals unexpected physiologic specificity in the JAK-STAT signaling pathway. PG-431-42. *Cell* 84: 431–442, 1996
47. Takeda K, Akira S: STAT family of transcription factors in cytokine-mediated biological responses. *Cytokine Growth Factor Rev* 11: 199–207, 2000
48. Tian WN, Braunstein LD, Apse K, Pang J, Rose M, Tian X, Stanton RC: Importance of glucose-6-phosphate dehydrogenase activity in cell death. *Am J Physiol* 276: C1121–C1131, 1999
49. Guijarro C, Egido J: Transcription factor-kappa B (NF-kappa B) and renal disease. *Kidney Int* 59: 415–424, 2001
50. Kawashima T, Murata K, Akira S, Tonozuka Y, Minoshima Y, Feng S, Kumagai H, Tsuruga H, Ikeda Y, Asano S, Nosaka T, Kitamura T: STAT5 induces macrophage differentiation of M1 leukemia cells through activation of IL-6 production mediated by NF-kappaB p65. *J Immunol* 167: 3652–3660, 2001
51. Marfaing-Koka A, Devergne O, Gorgone G, Portier A, Schall TJ, Galanaud P, Emilie D: Regulation of the production of the RANTES chemokine by endothelial cells: Synergistic induction by IFN-gamma plus TNF-alpha and inhibition by IL-4 and IL-13. *J Immunol* 154: 1870–1878, 1995
52. Finkel T: Reactive oxygen species and signal transduction. *IUBMB Life* 52: 3–6, 2001
53. Forman HJ, Torres M: Reactive oxygen species and cell signaling: Respiratory burst in macrophage signaling. *Am J Respir Crit Care Med* 166: S4–S8, 2002
54. Kaimori JY, Takenaka M, Nakajima H, Hamano T, Horio M, Sugaya T, Ito T, Hori M, Okubo K, Imai E: Induction of glia maturation factor-beta in proximal tubular cells leads to vulnerability to oxidative injury through the p38 pathway and changes in antioxidant enzyme activities. *J Biol Chem* 278: 33519–33527, 2003
55. Carter DC, Ho JX: Structure of serum albumin. *Adv Protein Chem* 45: 153–203, 1994
56. Lohse DL, Denu JM, Santoro N, Dixon JE: Roles of aspartic acid-181 and serine-222 in intermediate formation and hydrolysis of the mammalian protein-tyrosine-phosphatase PTP1. *Biochemistry* 36: 4568–4575, 1997
57. Abe J, Berk BC: Fyn and JAK2 mediate Ras activation by reactive oxygen species. *J Biol Chem* 274: 21003–21010, 1999

See related editorial, "Albumin Signals the Coming of Age of Proteinuric Nephropathy," on pages 504–505.

J Am Soc Nephrol 15: 1268–1276, 2004

Local Actions of Endogenous Angiotensin II in Injured Glomeruli

JI MA,*†‡ TAIJI MATSUSAKA,*‡ HAICHUN YANG,† HIROSHI KAWACHI,§ FUJIO SHIMIZU,§ YOSHITAKA ISAKA,¶ ENYU IMAI,¶ VALENTINA KON,‡ and IEKUNI ICHIKAWA*‡

**Department of Pediatrics, Tokai University School of Medicine, Isehara, Japan; †Division of Nephrology, Hua Shan Hospital, Fudan University, Shanghai, China; ‡Division of Pediatric Nephrology, Vanderbilt University Medical Center, Nashville, Tennessee; §Department of Cell Biology, Institute of Nephrology, Niigata University Graduate School of Medical and Dental Sciences, Niigata, Japan; ¶Division of Nephrology, Department of Internal Medicine and Therapeutics, Osaka University Graduate School of Medicine, Suita, Japan.*

Abstract. A previous study showed that exogenous angiotensin II (AngII) induces proliferation of glomerular cells through systemic actions of AngII. In the present study, the authors examined the mode of actions of endogenous AngII in injured kidneys that were made deficient in AT1 by using *in vivo* transfection of antisense oligodeoxynucleotide (AS-ODN). Thy-1 nephritis was induced in rats by injection of mAb 1-22-3. Four days later, glomerular transfection was performed by unilateral whole-kidney electroporation after AT1 AS-ODN delivery through the left renal artery ($n = 7$). The expression of renal AT1 was assessed by autoradiography. The effect of the AS-ODN transfection was assessed 3 d later and compared with transfection with control ODN ($n = 6$), systemically administered pharmacologic AT1 antagonist losartan ($n = 5$) as well as untreated Thy-1 animals ($n = 5$). Fluorescence-labeled AS-ODN was found transfected in almost all glomeruli and localized primarily to the mesangium. Compared with the contralateral untransfected kidney in both normal and Thy-1 rats, AS-ODN suppressed cortical AT1 expression by some 70%. The AS-ODN transfected kidneys of Thy-1 rats had significantly lower glomerular mesangial cell proliferation (7.38 ± 0.68 cells/glomerulus) and extracellular matrix accumulation (0.262 ± 0.009) than kidneys transfected with control ODN (10.94 ± 0.51 cells/glomerulus and 0.342 ± 0.031), contralateral untransfected kidneys (9.56 ± 1.01 cells/glomerulus and 0.371 ± 0.011), or kidneys that were exposed to Thy-1 alone (10.45 ± 1.06 cells/glomerulus and 0.359 ± 0.013). There were no significant differences in systolic BP among groups. In glomeruli, immunohistochemistry detected no difference in AT2 receptor expression, number of ED1-positive macrophages or number of apoptotic cells among groups. Thus, in renal injury induced by Thy-1 nephritis, selective suppression of mesangial AT1 expression by AS-ODN significantly reduced mesangial cell proliferation and matrix. These data provide *in vivo* evidence that injured glomeruli are sensitive to local tissue actions of AngII, which promote proliferation and matrix accumulation within the glomerulus.

Angiotensin II (AngII) is considered as one of the major profibrotic factors in tissue remodeling process. Through its type 1 receptor (AT1), AngII promotes cell proliferation and accumulation of extracellular matrix (ECM), resulting in renal and cardiac fibrosis (1,2). Experiments with AngII or AT1 antagonists have suggested that the effects of AngII on the kidney can be local, *i.e.*, through its receptor on renal cells, or systemic, *i.e.*, through its hypertensive effects (3). Differentiation of local *versus* systemic effects of AngII has relied primarily upon spot measurements of systemic BP. Serious questions have been raised regarding the representativeness of these spot measurements (4–6). Recently a chimeric mouse model has been developed that is made up with two types of cells: one with intact, the other with disrupted AT1 receptor gene. This model provided a unique opportunity to assess the local effects of AngII, as local AngII can act only through cells with intact AT1 receptors (2). Our study revealed that continuous infusion of AngII into AT1 chimeric mice causes similar glomerular cell proliferation regardless of the genotype of cells constituting the glomerulus. Instead, the degree of glomerular cell proliferation correlated with the level of systemic BP (7). This observation suggested that, at least in intact glomeruli, AngII acts primarily through its effects on systemic mechanism(s).

While systemic actions of AngII predominate over local effects in normal kidneys, there is reason to suspect that local AngII actions may prevail in injured kidneys. Thus, pharmacologic blockade of AngII cascade has been shown to attenuate glomerular damage independent of BP in some disease condi-

Received August 22, 2003. Accepted February 23, 2004.
Correspondence to Dr. Ji Ma, Pediatric Nephrology, Vanderbilt University Medical Center, 1161 21st. Ave. S. MCN C4204, Nashville, TN 37232. Phone: 615-322-7416; Fax: 615-322-7929; E-mail: ji.ma@vanderbilt.edu

1046-6673/1505-1268
Journal of the American Society of Nephrology

DOI: 10.1097/01.ASN.0000125675.70674.0F

tions, including diabetic nephropathy, when the AngII level in the serum or tissues is not elevated (8–11).

Mouse is a useful species for *in vivo* genetic manipulation to study the role of a specific gene product in diseases. However, when compared with rats, mice have been found over the last decade to be far more resistant to developing experimental glomerular diseases (12). In this regard, the rat Thy-1 nephritis induced by anti-thymocyte antibody is characterized by mesangial proliferation that follows mesangiolysis, where AT1 antagonist and angiotensin-converting enzyme inhibitor (ACEI) can ameliorate the histologic changes and decrease the number of proliferating cells and matrix accumulation in the glomeruli (13,14). Using this rat model, therefore we have ascertained the potential local effects of AngII in injured kidneys. The glomerular AT1 was suppressed by unilateral renal transfection with AT1 antisense (AS) oligodeoxynucleotide (ODN). The effects of AT1 AS-ODN were compared with contralateral untransfected kidneys with intact AT1 as well as with kidneys transfected with control ODN.

Materials and Methods

Animals

All animal procedures were conducted after approval by the Animal Committee of Tokai University Medical School. Male Wistar rats (Clea Japan Inc., Tokyo) weighing 140 to 160 g were housed in pathogen-free environment with a 12-h light/dark cycle and had free access to standard rat chow and drinking water.

Oligodeoxynucleotide

The ODN (HPLC-purified, phosphothionated) were purchased from Espec Oligo Service (Tsukuba, Ibaragi, Japan). The sequences of the ODN were the same as those used in the studies by Ambühl *et al.* (15), which were antisense ODN for rat AT1 receptor (AT1 AS-ODN): 5'-TAA CTG TGC CTG CCA-3', sense ODN: 5'-TGG CAG GCA CAG TTA-3', and scrambled ODN: 5'- CTT ACT AGC CTA GGC-3'.

Transfection of ODN into the Kidney

In vivo transfection was performed as previously reported (16). Under pentobarbital anesthesia (50 mg/kg, intraperitoneally), the left kidney and renal artery were surgically exposed. A 24G catheter (Angiocath; Becton Dickinson, Sandy, UT) was inserted into the left renal artery and immobilized by an artery clamp. The left kidney was perfused with 0.7 to 1.5 ml buffered saline solution (BSS: 140 mM MaCl, 5.4 mM KCl, 10 mM Tris·Cl, pH 7.6) throughout. Either antisense or control ODN (50 μg in 500 μl of BSS) was injected, and the renal vein was clamped. The left kidney was sandwiched by a pair of oval-shaped electrodes, CUY-654C (Nepa Gene Co., Ichikawa, Chiba, Japan). Three rectangular electric pulses (75 V, 0.1-s duration, 0.9-s interval) followed by another three pulses in opposite direction of electric field were delivered using a pulse generator, CUY-21 (Nepa Gene Co.). After the procedure, the catheter was removed and the puncture was closed with superglue. The total duration of ischemia in the left renal artery was <8 min.

Localization of Transfected ODN

FITC-labeled AS-ODN was used to localize the transfected ODN in the kidney. The kidney was harvested 10 min after reperfusion of the kidney, embedded in OTC compound, and frozen. Frozen sections were cut at 6-μm thickness to microscopically identify the specific fluorescence. The same section was then stained with 1:5000 mouse anti-OX-7 antibody (Chemicon, Temecula, CA) (16), visualized by rhodamine-conjugated rabbit anti-mouse IgG (Chemicon). Thus, transfected nuclei and glomerular mesangial area were observed as green and red, respectively. The pictures taken for green and red fluorescence of the same field were merged to evaluate the co-localization of the transfected nuclei and glomerular mesangial cells.

Quantification of AT1 and AT2 by Ang Binding Autoradiography

In each rat, the kidney transfected with ODN and the contralateral kidney were dissected in a longitudinal plane containing the papilla and frozen in the same block. The Ang binding autoradiography was performed as previously reported (2). Frozen sections (6 μm) were air dried for 1 h, pre-incubated with a binding buffer (5 mM Na_2EDTA, 0.005% bacitracin, 0.2% BSA in PBS) for 15 min. The slides were incubated in the binding buffer containing 0.5 nM [^{125}I]-Sar^1-Ile^8-AngII (NEN Life Science Products, Boston, MA) only (for total angiotensin receptors binding), or with 3 μM PD123319 (Sigma, St. Louis, MO), an AT2 antagonist (for AT1 binding), or with 3 μM losartan (Merck, Whitehouse Station, NJ), an AT1 antagonist (for AT2 binding), or with 3 μM Sar^1-Ile^8-AngII (for nonspecific binding) at room temperature for 2 h. Thereafter, the slides were washed in ice-cold 10 mM Tris·Cl (pH 7.6) four times, then in ice-cold distilled water two times, followed by air-drying for 2 h. The slides were exposed to a phosphorimaging plate, and the radioactive signal was visualized. Quantitative analysis was performed within the same section by using a computer image analysis system, BAS-5000 (Fujifilm, Tokyo, Japan).

Induction of Anti-Thy-1 Antibody Glomerulonephritis and Effects of Losartan

Due to the short duration of the efficiency of transfected AS-ODN, this pilot study was performed to identify the best time window to examine the effects of AT1 AS-ODN on Thy-1 kidneys. On day 0, monoclonal anti-Thy-1 antibody 1-22-3 (mAb 1-22-3, 0.5 mg/0.5 ml of PBS) (17) was injected into rats through tail vein. Losartan, an AT1 antagonist, was given in drinking water (1 g/L) from day 1 (13). Rats were analyzed on days 3, 4, 5, 6, and 7 (n = 3 for each time point). For labeling the proliferating cells, 100 mg/kg body wt of bromodeoxyuridine (BrdU; Sigma) was injected intraperitoneally every 8 h one day before sacrifice (18). Kidneys were cut longitudinally, fixed in 4% buffered paraformaldehyde, and embedded into paraffin. The number of proliferating glomerular mesangial cells was counted on sections stained with both BrdU antibody and OX-7 antibody (detailed below).

Experimental Protocol

Pilot experiments with 1 g/L of losartan in drinking water showed that the histologic difference between treated and un-treated kidneys became appreciable after day 6. Binding assay suggested a short duration (3 to 4 d) of AT1 suppression by its antisense. Therefore, the experimental protocol was designed as follows. On day 0, mAb 1-22-3 was injected through the tail vein. Rats were then randomly allocated to four groups: (group I) treated with AS-ODN (n = 7); (group II) treated with control ODN (n = 6); (group III) treated with an AT1 antagonist losartan (n = 5); and (group IV) with no treatment (n = 5). In group I, the left kidney was transfected with AS-ODN on day 4. Similarly, rats in group II were transfected either with sense ODN (n = 3) or with scrambled ODN (n = 3) on day 4. The data from

sense and scrambled ODN-treated rats were very similar, therefore they were pooled and shown in a single group (15). The AT1 antagonist, losartan, was used as a positive control for the effects of AT1 antisense (group III). Losartan was started on day 3 and continued throughout the experimental study to ensure sufficient antagonism of AT1. The average intake was about 37 ml/d per rat; therefore, the dose of losartan is estimated to be 230 mg/kg per d.

In all rats, an osmotic mini-pump (Alzet model 1007D; Alza Co., Palo Alto, CA) containing 40 mg/ml BrdU was implanted subcutaneously (19) under pentobarbital anesthesia on day 4. Before sacrifice on day 7, BP was measured by a tail-cuff method using Softron BP-98A analyzer (Softron Co., Tokyo, Japan) in all rats.

For group I and II rats, both the transfected and the contralateral kidneys were harvested and longitudinally dissected into two parts. One part was fixed in 4% buffered paraformaldehyde and embedded in a paraffin block for histologic analyses. The other part was frozen in OCT compound for Ang binding autoradiography. For groups III and IV, only the left kidney was harvested and histologically analyzed.

Assessment for Glomerular Proliferating Mesangial Cells

For double immunostaining for OX-7 and BrdU, BrdU staining kit (Oncogene Research Products, San Diego, CA) was used combined with mouse anti-OX-7 antibody (Chemicon, Temecula, CA). Paraffin sections of 3-μm thickness were dewaxed, rehydrated in PBS, and quenched in 3% H_2O_2/methanol. After antigen retrieval procedure with 0.1% trypsin at 37°C for 25 min, the tissue was denatured by denature solution for 20 min and blocked by blocking reagent for 10 min (both supplied in BrdU staining kit). The sections were incubated in a 2:1 mixture of anti-BrdU antibody and diluted anti-OX-7 antibody (1:2000) for 2 h before incubation in biotinylated sheep anti-mouse immunoglobin (Amersham Biosciences, Buckinghamshire, UK) and peroxidase-conjugated avidin (Vector Laboratories, Burlingame, CA). Both BrdU and OX-7 were visualized by diaminobenzidine (DAB). The ratio of the primary antibodies resulted in more intense color for BrdU than for OX-7. The differences in the color intensity and localization (BrdU in nuclei and OX-7 in cytoplasm) readily distinguished each signal.

Assessment for Glomerular Apoptotic Cells

Apoptotic cells in paraffin-embedded kidney sections were assessed by using ApopTag Peroxidase *In Situ* Apoptosis Detection Kit (Serologicals, Norcross, GA), which is based on TUNEL technique (20,21). Briefly, after dewax and rehydration, tissue sections were pretreated with 2 μg/ml Proteinase K at room temperature for 10 min and followed by quenching with hydrogen peroxide. The sections were incubated in Working Strength TdT Enzyme at 37°C for 1 h, then in Anti-Digoxigenin Conjugate at room temperature for 30 min, and visualized by DAB.

Immunohistochemistry

For type IV collagen, after antigen retrieval procedure with 0.1% trypsin at 37°C for 25 min and quenching endogenous peroxidase with 0.3% H_2O_2 in methanol at room temperature for 20 min, paraffin sections were incubated in rabbit polyclonal antibody against collagen IV (Chemicon) diluted at 1:1000 and then in peroxidase-conjugated anti-rabbit antibody (DAKO, Carpinteria, CA), visualized by DAB, and counterstained with hematoxylin. Sections incubated in PBS, instead of the primary antibody, were served as negative control.

For AT2, paraffin sections were heated in 0.01 M sodium citrate buffer (pH 6.0) by microwave for 5 min × 3 times. Endogenous peroxidase was quenched with 0.3% H_2O_2/methanol for 20 min, followed by blocking with Power Block (BioGenex Laboratories, San Ramon, CA) for 15 min. Sections were incubated in 1:100 diluted goat polyclonal antibody against AT2 (Santa Cruz, Santa Cruz, CA) at 4°C overnight and then in 1:100 diluted anti-goat-HRP (DAKO) at room temperature for 30 min and visualized by DAB. Sections from rat embryo collected at E12.5 d were used as positive control.

Macrophage was identified by ED1 immunohistochemistry (22). After antigen retrieval treatment with microwave and quenching with hydrogen peroxide, Mouse IgG Vector Elite ABC Kit (Vector Laboratories) was used. The primary antibody was mouse anti-rat ED1 (Biosource International, Hopkinton, MA) diluted at 1:200 and was allowed to react with the antigen at 4°C overnight. Sections incubated in PBS instead of the primary antibody were served as negative control.

Glomerular Morphometric Analyses

The image analysis was carried out in a blind fashion. For all analyses, glomeruli in the upper and lower pole areas were not selected because a proper electric field was sometimes not formed in these marginal areas during the ODN transfection. Also, tangential glomerular sections (diameter less than 80 μm) were not analyzed.

Proliferation of Glomerular Mesangial Cells. In kidney sections doubly stained for BrdU and OX-7, 50 glomeruli were randomly chosen, and the numbers of cells doubly positive for BrdU and OX-7 were counted.

Glomerular Extracellular Matrix Deposition. Thirty glomeruli were randomly selected in kidney sections stained by Masson trichrome method, and their pictures were taken with 40× objective lens. A grid of fixed scale with the interval equivalent to 10 μm was displayed over each picture. The cross points of the grids colored blue and the total points within the glomerulus were counted. On average, 107 points were assessed for each glomerulus. The ratios of the number of blue points to the total points were determined in 30 glomeruli, and the average of the ratio was used to represent the glomerular extracellular matrix deposition.

Glomerular Deposition of Type IV Collagen. In kidney sections stained for type IV collagen, 30 glomeruli were randomly selected. Each glomerulus was scored, as described previously (11,13,17): 0, the ratio of collagen IV area/the total glomerular area <25%; 1, ≥25% and <50%; 2, ≥50% and <75%; 3, ≥75%. For confirmation of the score for each glomerulus, area positive for type IV collagen staining and the total glomerular area were measured by a computer program (Motic Med CMIAS, Beijing, China).

Macrophages and Apoptotic Cells in Glomeruli. To count the macrophages and apoptotic cells in glomeruli, at least 50 glomeruli were randomly selected from kidney sections stained with ED1 or labeled by TUNEL. The number of macrophages in glomeruli was expressed as the average number of ED1-positive cells per glomerulus, while the number of apoptotic cells in glomeruli was expressed as the average number of the TUNEL-positive cells per 100 glomeruli.

Statistical Analyses

Results are expressed as mean ± SEM. ANOVA was used to evaluate the statistical differences among groups. Paired t test was applied to assess the statistical differences between the ODN transfected kidneys and the contralateral kidneys from the same animal. Statistical significance was set at $P < 0.05$.

Results

Gene Transfer to Glomerular Cells

To study the local actions of AngII that are independent of systemic actions, we inhibited AT1 receptors in glomerular cells by electroporation-mediated gene transfer of antisense

ODN. To monitor the efficiency of gene transfer and to identify the cell type that incorporated the DNA, we first infused FITC-labeled AS-ODN into the left kidney of normal rats via the left renal artery and electroporated that kidney. Fluorescein signals were observed in almost all examined glomeruli in transfected kidneys although in variable degrees. No signal was detected in the contralateral kidney or other organs (data not shown). Signals were localized mostly in the nuclei of glomeruli with only occasional signals in interstitial cells. Within the glomerulus, the green fluorescence from FITC-AS-ODN accumulated primarily in nuclei surrounded by OX-7–positive mesangial cells shown in red. Because of the color merge, some transfected nuclei emitted yellow color, indicating transfected mesangial cells (Figure 1).

Change of AT1 and AT2 Receptors by AS-ODN in Normal Rats

We next examined whether AS-ODN transferred by electroporation can suppress the renal AT1. Normal rats were transfected with AS-ODN as described above, and the kidneys were harvested 1, 2, 3, 4, and 7 d after the transfection. Expression of AT1 protein was quantified by binding autoradiography using [^{125}I]-Sar^{1}-Ile^{8}-AngII in the presence of an AT2 antagonist, PD123319. Throughout the experiments, the AT1 level did not appreciably change in the contralateral kidneys. By contrast, the AT1 level in the kidney transfected with AS-ODN decreased, especially within the cortex. The ratio of AngII binding in the transfected kidney to that in the contralateral kidney was averaging 29.3 ± 2.7%, 35.0 ± 3.8%, 36.2 ± 3.1% (each $n = 3$) during the first 3 d after the transfection, respectively. The ratio increased to 61.8 ± 8.6% ($n = 3$) 4 d after, and to 102.1 ± 12.6% ($n = 3$) 7 d after transfection. Neither AT1 sense ODN nor scrambled ODN affected the AT1 binding in the transfected kidney, compared with the contralateral kidney. Overall, these studies showed that in normal rats, electroporation-mediated transfection with AS-ODN effectively decreased the cortical AT1 receptor for 3 d (Figure 2C). Autoradiography also showed a slight decrease in AT1 binding in renal medulla in normal rats transfected with AS-ODN. In addition, binding for AT2 in normal rat kidneys transfected with AS-ODN decreased slightly as well (Figure 2D). However, no difference in the binding for AT2 was detected because of weak baseline signal.

Effect of Losartan on Glomerular Mesangial Cell Proliferation in Thy-1 Rats at Different Time Points

A pilot study of AT1 suppression with AT1 antagonist losartan from day 1 showed that, by counting the double BrdU/OX-7–positive cells in the glomeruli, the average number of proliferating mesangial cells on day 3 was 0.012 ± 0.003 per glomerulus in losartan-treated rats *versus* 0.019 ± 0.004 in non-treated rats on day 3, 0.491 ± 0.082 *versus* 0.324 ± 0.075 on day 4, 0.488 ± 0.029 *versus* 0.540 ± 0.031 on day 5, 0.341 ± 0.055 *versus* 0.502 ± 0.043 on day 6, and 0.517 ± 0.037 *versus*. 1.44 ± 0.060 on day 7 ($n = 3$ for each time point). Thus, losartan-induced reduction in proliferating mesangial cells became remarkable after day 6.

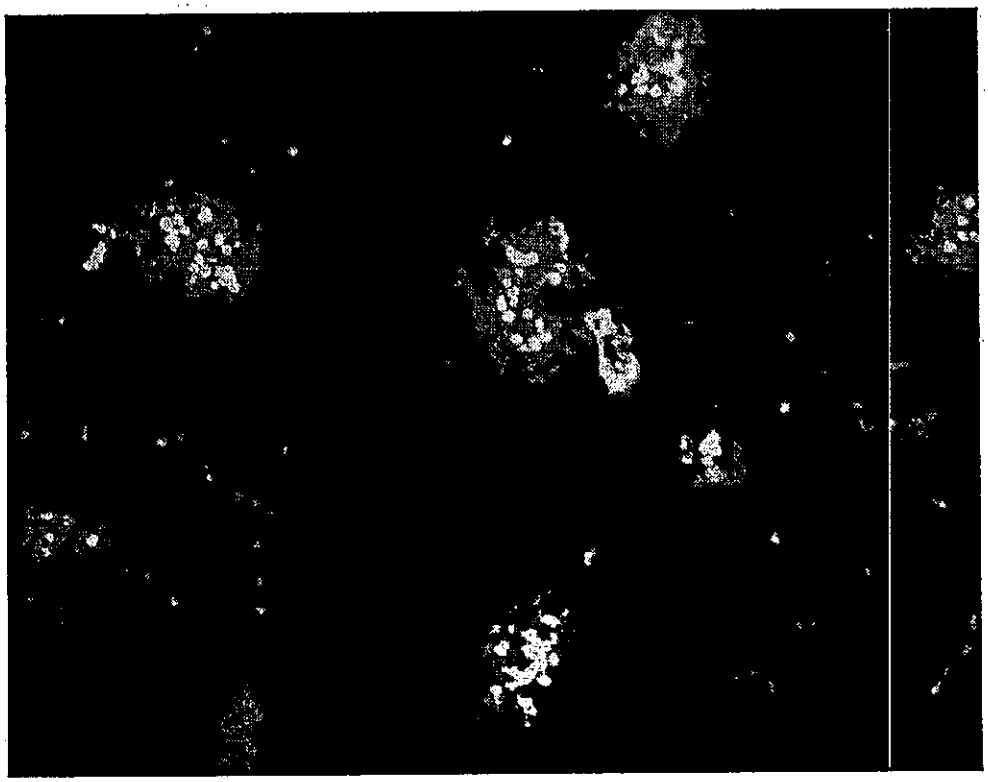

Figure 1. Localization of transfected oligodeoxynucleotide (ODN) in the kidney (×20). The kidney was excised 10 min after transfection with FITC-labeled ODN of angiotensin type 1 receptor (AT1) antisense. Glomerular mesangial area was stained in red by immunohistochemistry with anti-OX-7. Specific green FITC fluorescence showed that transfected ODN was localized mainly within the glomerular nuclei.

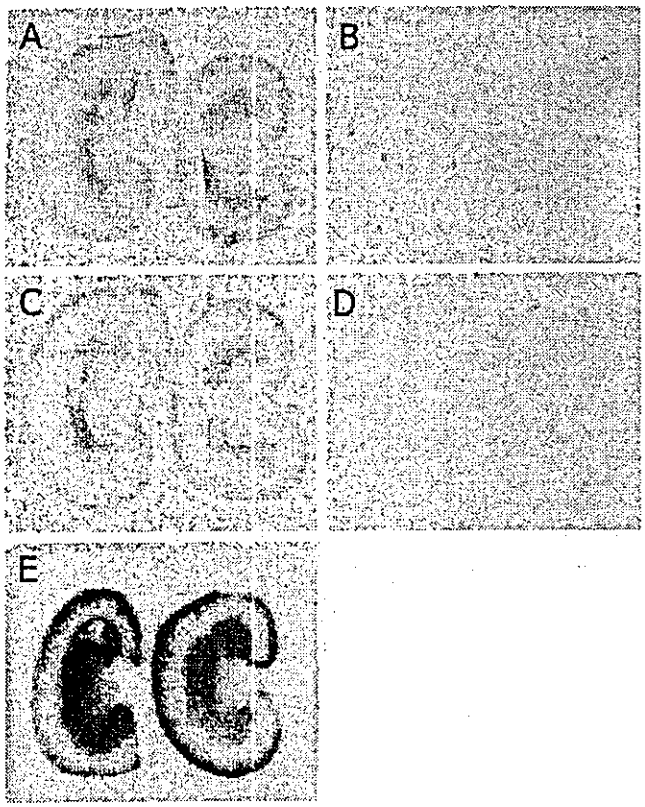

Figure 2. Autoradiography for AT1 and AT2. In normal rat (A–D) and rat with Thy-1 nephritis (E), binding for [^{125}I]-Sar^1-Ile^8-AngII was examined in the kidney transfected with AT1 phosphothionated antisense ODN (left kidney) and in the contralateral untransfected kidney (right kidney) 3 d after transfection. Specific AT1 binding in the cortex of transfected kidney was some 35% of that in the contralateral kidney in both normal (C) and Thy-1 (E) rats. (A) Autoradiography with [^{125}I]-Sar^1-Ile^8-AngII alone to show the total binding for AngII. (B) Autoradiography with [^{125}I]-Sar^1-Ile^8-AngII and nonlabeled Sar^1-Ile^8-AngII to show nonspecific binding. (C and E) Autoradiography with [^{125}I]-Sar^1-Ile^8-AngII and PD123319 to show specific AT1 binding. (D) Autoradiography with [^{125}I]-Sar^1-Ile^8-AngII and losartan to show specific AT2 binding.

Treatment of Anti-Thy-1 Antibody Nephritis with AS-ODN

We examined whether the local suppression of AT1 by this method can attenuate the cell proliferation, macrophage infiltration, and extracellular matrix (ECM) accumulation in anti-Thy-1 antibody-induced nephritis. On the basis of the time course of AT1 suppression observed in normal and Thy-1 rats, we performed ODN transfection 4 d after Thy-1 induction and analyzed tissues 3 d after the transfection.

The systolic BP measured at the end of the experiment was 135.6 ± 6.5 mmHg in group I (AS-ODN treated), 144.4 ± 4.4 in group II (Control-ODN treated), 119.4 ± 2.5 in group III (losartan-treated), and 141.7 ± 7.7 in group IV (not treated). BP in group III was lower than that in the other groups ($P < 0.05$). There was no difference in BP among the other three groups.

Similar to normal kidneys, transfection with AS-ODN significantly decreased AT1 in the kidneys with anti-Thy-1 nephritis. Thus, the cortical AT1 ascertained by binding autoradiography in transfected kidneys was on average 31.9 ± 2.0% ($n = 7$) of that in the contralateral kidneys (Figure 2E). Reduced binding of Ang in Thy-1 kidney occurred mainly in the cortex. The binding assay also revealed that the cortical AT1 was not evenly suppressed in the polar area of some kidneys, which was consistent with the more severe glomerular lesions seen on PAS-stained adjacent sections. By contrast, comparison with the contralateral kidneys revealed no difference in AT1 in the kidneys transfected with either sense ODN or scrambled ODN. In contrast to that in normal rat kidneys, transfection with AT1 AS-ODN in Thy-1 kidneys tended to increase medullary AT1 binding (Figure 2E). Immunohistochemistry was not able to show significant changes in the expression of AT2 receptor at day 7 in Thy-1 kidney treated or not treated with AT1 AS-ODN or losartan (data not shown).

Proliferating mesangial cells were detected by double staining for OX-7 and BrdU. The average number of proliferating mesangial cells were 10.45 ± 1.06 per glomerulus in the group IV (no treatment). Losartan treatment started on day 3 decreased the number of proliferating mesangial cells by some 50% (5.22 ± 0.95). In group I (AS-ODN treated), mesangial cell proliferation was 30% less in the transfected kidneys (7.38 ± 0.68) than the untreated nephritic kidneys. In group II, neither scrambled ODN nor sense ODN changed mesangial cell proliferation in the transfected or contralateral kidneys (Table 1, Figure 3). Only few glomerular apoptotic cells were detected by TUNEL method, averaging 5.94 ± 0.99 cells per 100 glomeruli; no significant difference was found among groups.

Immunohistochemistry with ED1 showed that there was no significant difference in the number of macrophages per glomeruli among the groups (AS-ODN transfected, 0.680 ± 0.094; AS-ODN contralateral untransfected, 0.757 ± 0.070; Control-ODN transfected, 0.737 ± 0.027; Control-ODN contralateral untransfected, 0.714 ± 0.025; losartan treated, 0.612 ± 0.072; Thy-1 untreated, 0.756 ± 0.086 cells/glomerulus; $P > 0.05$).

ECM accumulation was examined by point-counting analysis in Masson trichrome-stained sections. Losartan treatment reduced the ratio of blue points by 35%. In group I, ECM accumulation was significantly reduced by 37% in the transfected kidneys, but not in the contralateral kidneys. In group II, neither scrambled ODN nor sense ODN transfection affected ECM accumulation in the transfected or contralateral kidneys (Table 1, Figure 4). Similar results were observed in terms of glomerular collagen IV positive area (Figure 5).

Taken together, unilateral AS-ODN transfection of the kidney, which depleted AT1 receptor significantly, attenuated mesangial cell proliferation and glomerular ECM accumulation in Thy-1 nephritis.

Discussion

Glomerular transfection of AS-ODN for AT1 was successfully performed by renal artery injection followed by *in situ*

Table 1. Histopathological analyses of kidneys with anti-Thy-1 antibody nephritis

Group	*n*	No. of BrdU/OX-7 Double-Positive Cells per Glomerulus	Glomerular Deposition of ECM	Glomerular Deposition of Type IV Collagen
PS-AS-ODN, transfected	7	7.38 ± 0.68^{abc}	0.262 ± 0.009^{abc}	0.988 ± 0.065^{abc}
PS-AS-ODN, contralateral	7	9.56 ± 1.01	0.371 ± 0.011	1.357 ± 0.091
Control ODN, transfected	6	10.94 ± 0.51	0.342 ± 0.031	1.257 ± 0.096
Control ODN, contralateral	6	11.07 ± 0.84	0.362 ± 0.033	1.169 ± 0.046
Losartan-treated	5	5.22 ± 0.95^{a}	0.235 ± 0.014^{a}	0.429 ± 0.081^{a}
Thy-1 control	5	10.45 ± 1.06	0.359 ± 0.013	1.331 ± 0.063

[a] $P < 0.05$ compared with Thy-1 control.
[b] $P < 0.05$ compared with Control ODN, transfected.
[c] $P < 0.05$ compared with PS-AS-ODN, contralateral.

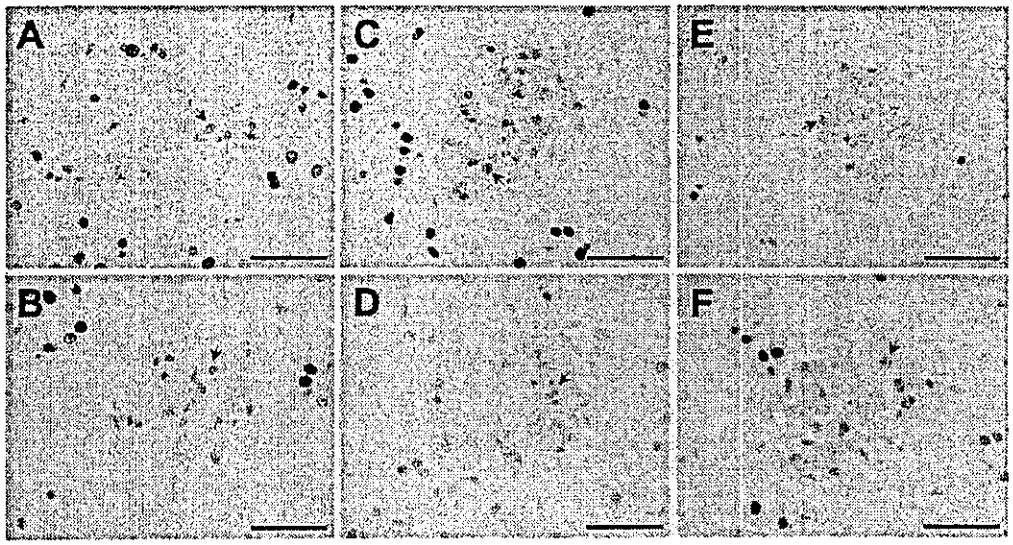

Figure 3. Proliferating glomerular mesangial cells in glomeruli with anti-Thy-1 antibody nephritis from different groups (×40). The number of proliferating glomerular mesangial cells detected by double immunohistochemical staining for OX-7 and incorporated BrdU in AT1 antisense oligodeoxynucleotide (ODN) transfected kidney with anti-Thy-1 antibody nephritis (A) was significantly less than that in the contralateral untransfected (B), the control ODN transfected (C), and the Thy-1 disease control (F) kidney. (A) Antisense ODN-transfected; (B) contralateral to the antisense ODN-transfected; (C) control ODN-transfected; (D) contralateral to the control ODN-transfected; (E) losartan-treated; (F) anti-Thy-1 antibody–treated alone. Black arrows indicate representative proliferating mesangial cells. Black scale bar, 50 μm.

kidney electroporation. Our experiments using FITC-labeled ODN showed that, almost all glomeruli incorporated ODN, which was localized mainly within mesangial cell nuclei. These findings were consistent with those by Tsujie *et al.* (16). The transfection efficiency of AT1 AS-ODN was determined by autoradiography of specific binding for [^{125}I]-Sar^{1}-Ile^{8}-AngII under the presence of an AT2 antagonist PD123319. One to three days after transfection, the specific binding of AT1 in the cortex of AS-ODN transfected kidneys was suppressed to some 30 to 35% of that in the contralateral untransfected kidneys. The AT1 binding recovered to approximately 60% of the contralateral level 4 d after, and near 100% 7 d after transfection. We applied the unilateral AS-ODN transfection methodology to test the hypothesis that, unlike intact glomeruli, injured glomeruli are sensitive to the local actions of AngII.

Anti-thymocyte nephritis is characterized by mesangial cell proliferation and ECM accumulation in the mesangium without major change in systemic BP (23–25). Within 20 to 28 h after the intravenous injection of antibody, intraglomerular mesangiolysis is complete and mesangial cell proliferation from the extraglomerular hilar area starts (24). Infiltration of macrophages into glomeruli appears 2 h after injection with Thy-1 antibody, and peaks at day 3 to day 7 (26). The peak of glomerular cell proliferation appears on day 6 to day 7, when the ECM accumulation in the glomeruli also becomes remarkable. The renal histologic changes gradually resolve over the next one to two weeks (24,27,28). In the glomerulus, AT1 receptor localized mainly in the mesangial cells (29–31). *In vitro* studies have shown that AngII causes mesangial cell proliferation and production of extracellular matrix (ECM)

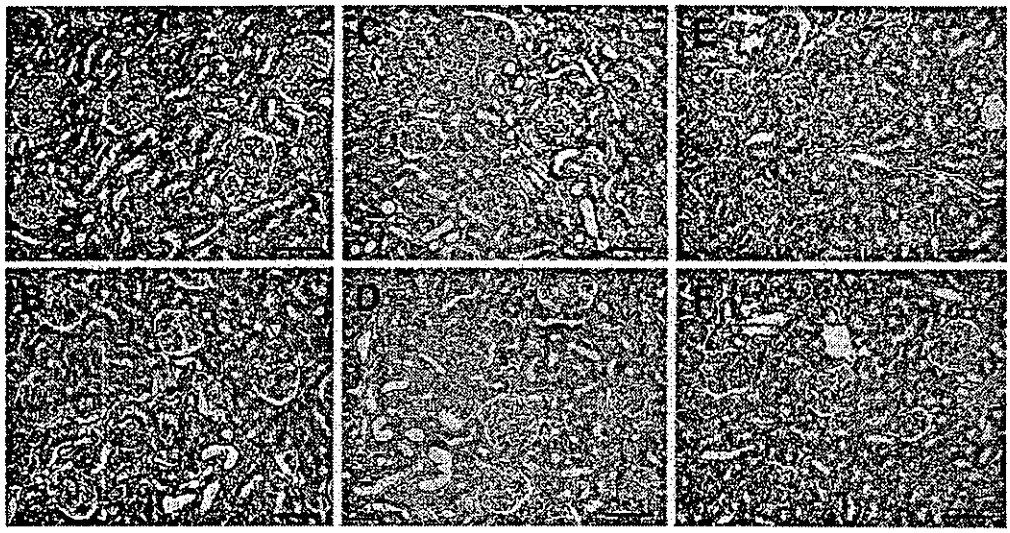

Figure 4. ECM deposition in glomeruli with anti-Thy-1 antibody nephritis from different groups (×20). Masson trichrome staining showed significantly less deposition of glomerular matrix in AT1 antisense ODN–transfected kidney with Thy-1 nephritis (A) compared with that of the contralateral untransfected (B), the control ODN-transfected (C), and the Thy-1 disease control (F) kidney. (A) antisense ODN-transfected; (B) contralateral to the antisense ODN-transfected; (C) control ODN-transfected; (D) contralateral to the control ODN-transfected; (E) losartan-treated; (F) anti-Thy-1 antibody–treated alone. Black scale bar, 100 μm.

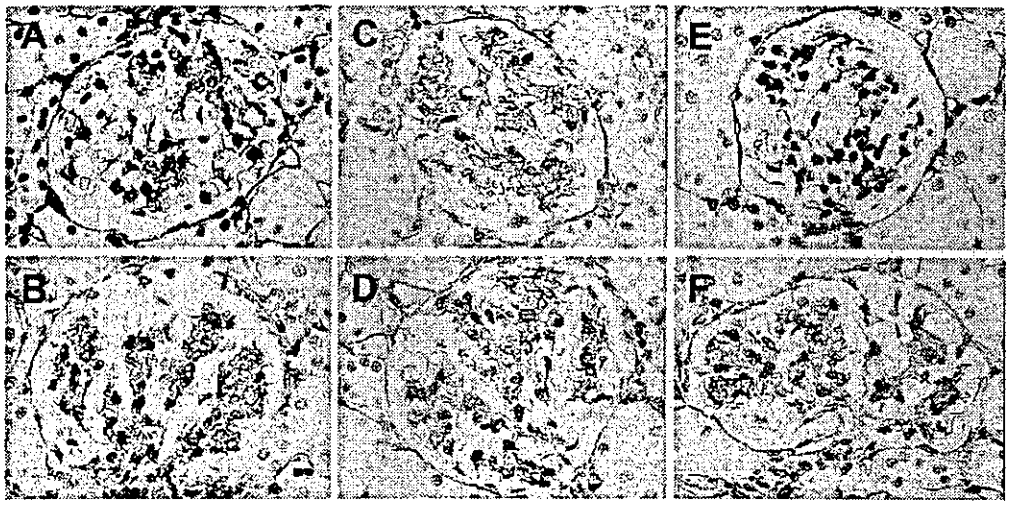

Figure 5. Accumulation of type IV collagen in glomeruli with anti-Thy-1 antibody nephritis from different groups (×40). Immunohistochemical study for type IV collagen demonstrated significantly less accumulation of type IV collagen in AT1 antisense ODN transfected kidney with Thy-1 nephritis (A) compared with that of the contralateral untransfected (B), the control ODN transfected (C), and the Thy-1 disease control (F) kidney. (A) antisense ODN-transfected; (B) contralateral to the antisense ODN-transfected; (C) control ODN-transfected; (D) contralateral to the control ODN-transfected; (E) losartan-treated; (F) anti-Thy-1 antibody treated alone.

through its AT1 receptor (32). In Thy-1 nephritis, AT1 antagonist or ACEI has been shown to ameliorate the above glomerular pathologic changes (13,23,25). When the AT1 AS-ODN was transfected to the Thy-1 kidney on day 4, the specific binding for AT1 in the renal cortex was suppressed by some 70% compared with the contralateral untransfected kidney on day 7. Moreover, our pilot experiments showed that, there is no difference in the number of proliferating mesangial cells between losartan-treated and untreated Thy-1 kidneys until day 6. Therefore, we set the protocol to unilaterally transfect Thy-1 kidneys with AT1 AS-ODN on day 4 and to compare between the antisense transfection and control ODN on day 7.

Selective suppression of renal AT1 by transfection with AS-ODN resulted in significantly fewer proliferating glomerular mesangial cells when compared to control ODN, as identified by BrdU and OX-7 double-positive cells. Moreover, the amount of ECM accumulation assessed by Masson trichrome

and collagen IV stainings was also significantly reduced by AS-ODN transfection on day 7. In glomeruli, no significant change was detected in infiltrating macrophages after AT1 antisense transfection or losartan administration. This may reflect the relatively late experimental intervention (starting at day 4) or assessment (at day 7) (22,33). Nevertheless, appreciable decrease was found in the number of macrophages in Thy-1 glomeruli after AT1 blockade either locally by AS-ODN transfection or systemically by losartan administration.

Previous studies have attempted to distinguish the effects of local *versus* systemic AngII in renal disease (3,4,17,34,35). However, while accurate measurements of systemic BP can ascertain change in this parameter, BP is but one potentially important systemic mechanism; others include aldosterone, adrenergic system, and other neuro-humoral factors. Some investigators employed a method of delivering AngII, AT1 antagonist, or ACEI unilaterally via the renal artery to test the local action of AngII. However, immediate escape into the systemic circulation and the delayed elimination of the peptide or drug made the selective blockade at the kidney level incomplete (36,37) and distinguishing systemic *versus* local effects difficult. In the present study, the unilateral electroporation that follows ipsilateral injection of DNA was designed to confine the AngII effect to one kidney. Using this method of selectively inhibiting unilateral AT1 functions, we demonstrate that in glomeruli injured by anti-thymocyte antibody, AngII promotes local glomerular cell proliferation and ECM accumulation through the local AT1 receptors.

Thy-1 nephritis is not a model characterized by hypertension (14,18,24,27,38,39), and treatment with conventional antihypertensive agents does not protect glomeruli from injury (17,24). Nevertheless, in view of the sporadic nature of the BP measurements made in these studies, the potential influence of systemic BP on Thy-1 kidney remains conceivable. In the present study, the AT1 antagonist losartan given orally had more renal protection than antisense transfection. This difference may be attributed to losartan's BP-lowering effect and/or to its more complete suppression of the AT1 receptor within the diseased kidney. It is also possible that, when given orally, losartan may have other systemic (besides BP) effects that modulate the glomerular lesion of this model. With this caveat, the present study has demonstrated that local injurious actions of AngII are involved in glomerular disease. In this connection, a significant upregulation of the AT1 gene activity and protein has been documented in rat glomeruli following anti-Thy-1 antibody injection (8), supporting the idea that injured glomeruli are more susceptible to locally acting AngII. Moreover, unlike our earlier study on chimeric mice given AngII infusion exogenously, the active AngII in the present study is of endogenous origin. Therefore, the results from the present study using the antisense DNA transfection methodology have also validated the notion that the renoprotective effect of pharmacologic inhibition found by others can be attributed to the suppression of endogenous AngII actions.

Regarding the nature of local AngII effect, one might speculate that expression of angiotensin type 2 receptor (AT2) is affected in Thy-1 kidneys and even more so after blockade of AT1 (40), which may in turn have mediated the protective effects seen in this study. In view of the markedly low expression level of AT2 in Thy-1 glomeruli examined in the present study, the contribution of AT2 to our findings appears insignificant. Likewise, the potential role of apoptosis in Thy-1 glomeruli remains unknown due to its low baseline level (41).

Autoradiography showed that the medullary expression of AT1 tended to decrease in normal kidney while increase in Thy-1 kidney after transfection in an unexplainable manner. It remains unclear if those changes have any effect on glomeruli.

The local action of AngII on the Thy-1 kidney may be of hemodynamic or non-hemodynamic nature (13,17,26,42–44). The present study is not designed to ascertain the relative contribution of these factors.

In summary, AngII of endogenous origin promotes mesangial cell proliferation and ECM accumulation in an injury model of glomerulonephritis through its action on the local AT1 receptor.

Acknowledgments

This work was supported by Research for the Future Program of Japan Society for the Promotion of Science, the National Institutes of Health grants DK-44757 and DK-37868, and grants from Ministry of Education of China (81038) and Shanghai Education Commission (SG-01008).

References

1. Matsusaka T, Hymes J, Ichikawa I: Angiotensin in progressive renal diseases: Theory and practice. *J Am Soc Nephrol* 7: 2025–2043, 1996
2. Matsusaka T, Katori H, Inagami T, Fogo A, Ichikawa I: Communication between myocytes and fibroblasts in cardiac remodeling in angiotensin chimeric mice. *J Clin Invest* 103: 1451–1458, 1999
3. Lafayette RA, Mayer G, Park SK, Meyer TW: Angiotensin II receptor blockade limits glomerular injury in rats with reduced renal mass. *J Clin Invest* 90: 766–771, 1992
4. Bidani AK, Griffin KA, Bakris G, Picken MM: Lack of evidence of blood pressure-independent protection by renin-angiotensin system blockade after renal ablation. *Kidney Int* 57: 1051–1661, 2000
5. Griffin KA, Abu-Amarah I, Picken M, Bidani AK: Renoprotection by ACE inhibition or aldosterone blockade is blood pressure-dependent. *Hypertension* 41: 201–206, 2003
6. Kurtz TW: False claims of blood pressure independent protection by blockade of the renin angiotensin aldosterone system. *Hypertension* 41: 193–196, 2003
7. Takaya J, Matsusaka T, Katori H, Fogo A, Ichikawa I: Systemic angiotensin has no local impact on the DNA synthesis in the glomerulus in vivo [Abstract]. *J Am Soc Nephrol* 11: 372A, 2000
8. Dechow C, Morath C, Peters J, Lehrke I, Waldherr R, Haxsen V, Ritz E, Wagner J: Effects of all-trans retinoic acid on renin-angiotensin system in rats with experimental nephritis. *Am J Physiol Renal Physiol* 281: F909–F919, 2001
9. Ballermann BJ, Skorecki KL, Brenner BM: Reduced glomerular angiotensin II receptor density in early untreated diabetes mellitus in rat. *Am J Physiol* 247: F110–F116, 1984
10. Wilkes BM: Reduced glomerular antiotensin II receptor density in diabetes mellitus in the rat: Time course and mechanism. *Endocrinology* 120: 1291–1298, 1987

11. O'Brien RC, Cooper ME, Jerums G, Doyle AE: The effects of perindopril and triple therapy in a normotensive model of diabetic nephropathy. *Diabetes* 42: 604–609, 1993
12. Ma L-J, Fogo A: Model of robust induction of glomerulosclerosis in mice: Importance of genetic background. *Kidney Int* 64: 350–5, 2003
13. Peters H, Border WA, Noble NA: Targeting TGF-beta overexpression in renal disease: Maximizing the antifibrotic action of angiotensin II blockade. *Kidney Int* 54: 1570–1580, 1998
14. Nakamura T, Obata J, Kimura H, Ohno S, Yoshida Y, Kawachi H, Shimizu F: Blocking angiotensin II ameliorates proteinuria and glomerular lesions in progressive mesangioproliferative glomerulonephritis. *Kidney Int* 55: 877–889, 1999
15. Ambühl P, Gyurko R, Phillips MI: A decrease in angiotensin receptor binding in rat brain nuclei by antisense oligonucleotides to the angiotensin AT1 receptor. *Regulatory Peptides* 59: 171–182, 1995
16. Tsujie M, Isaka Y, Nakamura H, Imai E, Hori M: Electroporation-mediated gene transfer that targets glomeruli. *J Am Soc Nephrol* 12: 949–954, 2001
17. Cheng QL, Orikasa M, Morioka T, Kawachi H, Chen XM, Oite T, Shimizu F: Progressive renal lesions induced by administration of monoclonal antibody 1-22-3 to unilaterally nephrectomized rats. *Clin Exp Immunol* 102: 181–185, 1995
18. Miyazaki Y, Tsuchida S, Nishimura H, Pope JC 4th, Harris RC, Mckanna JM, Inagami T, Hogan BL, Fogo A, Ichikawa I: Angiotensin induces the urinary peristaltic machinery during the perinatal period. *J Clin Invest* 102: 1489–1997, 1998
19. van Krimpen C, Smits JF, Cleutjens JP, Debets JJ, Schoemaker RG, Struyker-Boudier HA, Bosman FT, Daemen MJ: DNA synthesis in the non-infarcted cardiac interstitium after left coronary artery ligation in the rat: effects of captopril. *J Mol Cell Cardiol* 23: 1245–1253, 1991
20. Gavrieli Y, Sherman Y, Ben-Sasson SA: Identification of programmed cell death in situ via specific labeling of nuclear DNA fragmentation. *J Cell Biol* 119: 493–501, 1992
21. Thomas GL, Yang B, Wagner BE, Savill J, El Nahas AM: Cellular apoptosis proliferation in experimental renal fibrosis. *Nephrol Dial Transplant* 13: 2216–2226, 1998
22. Yoshimura A, Inui K, Nemoto T, Uda S, Sugenoya Y, Watanabe S, Yokota N, Taira T, Iwasaki S, Ideura T: Simvastatin suppresses glomerular cell proliferation and macrophage infiltration in rats with mesangial proliferative nephritis. *J Am Soc Nephrol* 9: 2027–2039, 1998
23. Kiyama S, Nanishi F, Tomooka S, Okuda S, Onoyama K, Fujishima M: Inhibitory effects of antihypertensive drugs on mesangial cell proliferation after anti-thymocyte serum (ATS)-induced mesangiolysis in spontaneously hypertensive rats. *Life Sci* 54: 1891–1900, 1994
24. Hugo C, Shankland SJ, Bowen-Pope DF, Couser WG, Johnson RJ: Extraglomerular origin of the mesangial cell after injury. A new role of the juxtaglomerular apparatus. *J Clin Invest* 100: 786–794, 1997
25. Zoja C, Abbate M, Corna D, Capitanio M, Donadelli R, Bruzzi I, Oldroyd S, Benigni A, Remuzzi G: Pharmacologic control of angiotensin II ameliorates renal disease while reducing renal TGF-beta in experimental mesangioproliferative glomerulonephritis. *Am J Kidney Dis* 31: 453–463, 1998
26. Kobayashi H, Orikasa M, Naito M, Kawasaki K, Oite T, Kawachi H, Yamashita A, Takeya M, Nihei H, Shimizu F: Detailed analysis of phenotypes of macrophages infiltrating glomeruli in rat anti-Thy-1 nephritis. *Nephron* 77: 333–339, 1997
27. Okuda S, Languino LR, Ruoslahti E, Border WA: Elevated expression of transforming growth factor-beta and proteoglycan production in experimental glomerulonephritis. Possible role in expansion of the mesangial extracellular matrix. *J Clin Invest* 86: 453–462, 1990
28. Wakasugi M, Kawachi H, Omori S, Takagi J, Nishi S, Arakawa M, Shimizu F: Expression of the molecule detectable by anti-propolypeptide of von Willebrand factor antibody in rat mesangial cells in anti-Thy 1.1 mAb 1-22-3 induced glomerulonephritis: A marker of injured mesangial cells. *Nephron* 82: 338–47, 1999
29. Paxton WG, Runge M, Horaist C, Cohen C, Alexander RW, Bernstein KE: Immunohistochemical localization of rat angiotensin II AT1 receptor. *Am J Physiol* 264: F989–F995, 1993
30. Harrison-Bernard LM, Navar LG, Ho MM, Vinson GP, el-Dahr SS: Immunohistochemical localization of ANG II AT1 receptor in adult rat kidney using a monoclonal antibody. *Am J Physiol* 273: F170–F177, 1997
31. Kakinuma Y, Fogo A, Inagami T, Ichikawa I: Intrarenal localization of angiotensin II type 1 receptor mRNA in the rat. *Kidney Int* 43: 1229–1235, 1993
32. Wolf G, Neilson EG: Angiotensin II as a renal growth factor. *J Am Soc Nephrol* 3: 1531–1540, 1993
33. Panzer U, Schneider A, Wilken J, Thompson DA, Kent SB, Stahl RA: The chemokine receptor antagonist AOP-RANTES reduces monocyte infiltration in experimental glomerulonephritis. *Kidney Int* 56: 2107–2115, 1999
34. Taal MW, Chertow GM, Rennke HG, Gurnani A, Jiang T, Shahsafaei A, Troy JL, Brenner BM, Mackenzie HS: Mechanisms underlying renoprotection during renin-angiotensin system blockade. *Am J Physiol Renal Physiol* 280: F343–F355, 2001
35. Raij L, Chiou XC, Owens R, Wrigley B: Therapeutic implications of hypertension-induced glomerular injury. Comparison of enalapril and a combination of hydralazine, reserpine, and hydrochlorothiazide in an experimental model. *Am J Med* 79: 37–41, 1985.
36. Hamilton TA, Handa RK, Harding JW, Wright JW: A role for the angiotensin IV/AT4 system in mediating natriuresis in the rat. *Peptides* 22: 935–944, 2001
37. Miller MJ, Scroop GC: Disappearance of angiotensin II and noradrenaline from the renal and femoral circulations of the dog. *Clin Sci (Lond)* 58: 29–35, 1980
38. Wenzel UO, Thaiss F, Helmchen U, Stahl RAK, Wolf G: Angiotensin II infusion ameliorates the early phase of a mesangioproliferative glomerulonephritis. *Kidney Int* 61: 1020–1029, 2002
39. Wenzel UO, Thaiss F, Panzer U, Schneider A, Schwietzer G, Helmchen U, Stahl RA: Effect of renovascular hypertension on experimental glomerulonephritis in rats. *J Lab Clin Med* 134: 292–303, 1999
40. Ruiz-Ortega R, Esteban V, Suzuki Y, Ruperez M, Mezzano S, Ardiles L, Justo P, Ortiz A, Egido J: Renal expression of angiotensin type 2 (AT2) receptors during kidney damage. *Kidney Int* 64: S21–S26, 2003
41. Shimizu A, Kitamura H, Masuda Y, Ishizaki M, Sugisaki Y, Yamanaka N: Apoptosis in the repair process of experimental proliferative glomerulonephritis. *Kidney Int* 47: 114–121, 1995
42. Kanai H, Okuda S, Kiyama S, Tomooka S, Hirakata H, Fujishima M: Effects of endothelin and angiotensin II on renal hemodynamics in experimental mesangial proliferative nephritis. *Nephron* 64: 609–614, 1993
43. Ostendorf T, Kunter U, van Roeyen C, Dooley S, Janjic N, Ruckman J, Eitner F, Floege J: The effects of platelet-derived growth factor antagonism in experimental glomerulonephritis are independent of the transforming growth factor-beta system. *J Am Soc Nephrol* 13: 658–667, 2002
44. Haraguchi M, Border WA, Huang Y, Noble NA: t-PA promotes glomerular plasmin generation and matrix degradation in experimental glomerulonephritis. *Kidney Int* 59: 2146–2155, 2001

J Am Soc Nephrol 15: 2383–2390, 2004

CCAAT/Enhancer-Binding Protein δ Contributes to Myofibroblast Transdifferentiation and Renal Disease Progression

MASANOBU TAKEJI,*† NORITAKA KAWADA,*† TOSHIKI MORIYAMA,*‡ KATSUYUKI NAGATOYA,* SUSUMU OSETO,* SHIZUO AKIRA,§ MASATSUGU HORI,* ENYU IMAI,* and TAKESHI MIWA†

**Department of Internal Medicine and Therapeutics, Graduate School of Medicine, Osaka University, Suita, Osaka, Japan; †Genome Information Research Center, Osaka University, Suita, Osaka, Japan; ‡School of Health and Sport Sciences, Osaka University, Toyonaka, Osaka, Japan; and §Research Institute for Microbial Diseases, Osaka University, Suita, Osaka, Japan*

Abstract. Myofibroblasts are pivotal participants in pathologic processes in a wide variety of organs, such as lung, liver, and kidney, by producing several inflammatory cytokines and extracellular matrices. The mechanism by which transdifferentiation from original cell to myofibroblast occurs, however, is still unclear. The expression of smooth muscle α-actin (SMαA) is the most characteristic feature of myofibroblasts; therefore, it was speculated that any factors that promote SMαA expression might be the key to transdifferentiation to myofibroblasts and disease exacerbation. A transcription factor CCAAT/enhancer-binding protein δ (C/EBPδ) was identified and demonstrated to bind to sequences including the CArG motif from SMαA intron 1 and to increase transcriptional activity of this promoter. Expression of SMαA and C/EBPδ in the glomerular area was upregulated in rat anti-Thy1 glomerulonephritis and mouse Habu-venom glomerulonephritis, both of which are models of mesangioproliferative glomerulonephritis. In the latter model, C/EBPδ knockout mice demonstrated significantly less SMαA expression in the glomerular area on day 8 and less renal functional deterioration on day 14, compared with wild-type mice. These data suggest an important role for C/EBPδ in myofibroblast transdifferentiation and glomerulonephritis exacerbation.

Tissue injury and sustained abnormal repair processes after initial insults are the major causes of tissue fibrosis leading to end-stage organ failure in many tissues, including lung, liver, and kidney (1,2). One of the common histopathologic features of fibrosis is an early emergence of myofibroblasts, a unique mesenchymal cell population with ultrastructural properties of both muscle and nonmuscle cells. Myofibroblasts express smooth muscle cytoskeletal markers, such as smooth muscle α-actin (SMαA), caldesmon, and desmin, and actively produce inflammatory cytokines and extracellular matrices. They are thought to be central participants in wound healing, presumably as an extension or accentuation of their role in normal growth and differentiation. In contrast, uncontrolled generation or activation of myofibroblasts results in excessive formation of granulation tissue and accumulation of extracellular matrices, leading to tissue fibrosis and eventual organ function loss (2,3).

Numerous types of cells have been characterized as the source of myofibroblasts, including pericytes, hepatic stellate cells, mesangial cells, interstitial cells, and granulation tissue fibroblasts. However, the molecular mechanism of myofibroblast formation and of expression of smooth muscle cytoskeletal markers and matrix proteins in these cells have not been well characterized. We have been investigating the pathophysiologic significance of myofibroblasts in renal disease. Both caldesmon and SMαA are sensitive and useful molecular markers for myofibroblasts in progressive renal disease (4,5). Emergence of SMαA-expressing myofibroblasts has been documented, focusing on prognostic value in IgA nephropathy (6) and other types of glomerulonephritis (7–9), diabetic nephropathy (10), and chronic allograft nephropathy in posttransplant patients (11). These observations in human renal disease highlight the significance of myofibroblasts in progressive renal disease; therefore, many experimental investigations use myofibroblast expansion as a marker of disease progression and its suppression as a marker of therapeutic efficacy.

We aim to elucidate the molecular mechanisms of SMαA gene regulation during myofibroblast formation. Intronic CArG motif is essential for the transcriptional activation of SMαA gene in both smooth muscle cells (12) and renal myofibroblasts (13). Although serum response factor (SRF) is a well-known binding factor for the CArG motif, it is distributed

Received September 8, 2003. Accepted May 27, 2004.
Correspondence to Dr. Toshiki Moriyama, Department of Internal Medicine and Therapeutics, Graduate School of Medicine, Osaka University, 2-2 Yamadaoka, Suita, Osaka, 565-0871, Japan. Phone: +81-6-6879-3632; Fax: +81-6-6879-3639; E-mail: moriyama@medone.med.osaka-u.ac.jp
M.T. and N.K. contributed equally to this work.
N.K.'s current affiliation is Center for Hypertension and Renal Disease Research, Georgetown University Medical Center, Washington, DC.
1046-6673/1509-2383
Journal of the American Society of Nephrology

DOI: 10.1097/01.ASN.0000136426.01160.2F

ubiquitously in various cells. Therefore, it is likely that any other transcription factors bind to this region to enhance SMαA expression and might contribute to production of inflammatory cytokines and extracellular matrices. We report here the molecular identification and characterization of transcription factor CCAAT/enhancer-binding protein δ (C/EBPδ) that binds to sequences that include the CArG motif from intron 1 of the SMαA gene. C/EBPδ enhances SMαA expression and also contributes to the production of proinflammatory chemokine leading to renal disease progression.

Materials and Methods

Animals and Cultured Cells

C/EBPδ-deficient (C/EBPδ[−/−]) mice and wild-type (C/EBPδ[+/+]) mice were generated by mating C/EBPδ heterozygous (C/EBPδ[+/−]) mice (background strain 129) (14). Sprague-Dawley rats were purchased from Japan SLC, Inc. (Hamamatsu, Japan). Primary cultured mesangial cells were obtained from C/EBPδ(−/−) mice and C/EBPδ(+/+) mice as described previously (15). Mesangial cells were cultured in RPMI 1640 medium (Life Technologies BRL, Rockville, MD) with 20% FCS (Life Technologies BRL). Mouse NIH-3T3 fibroblasts were cultured in DMEM with 10% FCS, penicillin G (100 U/ml), and streptomycin (100 μg/ml).

Yeast One-Hybrid Analysis

To identify factors that bind to DNA sequences including the CArG motif from SMαA intron 1, we used a yeast one-hybrid system. Two oligonucleotides, 5'-AATTCGTTTTACCTAATTA*T*GAAATGTTT-TACCTAATTA*T*GAAATGTTTTACCTAATTA*T*GAAATGA-3' and 5'-AATTTCATTTCATAATTAGGTAAAACATTTCATAATT-AGGTAAAACATTTCATAATTAGGTAAAACG-3', that contained three tandem repeats of the 20-bp CArG motif at bp + 1098 of SMαA intron 1, with one point mutation (G to T and C to A; italics) to avoid SRF binding were synthesized, annealed, and inserted upstream of the E1b minimal promoter in pHISi-1 (named pHISi-3CArGM) and the CYC1 minimal promoter in pLacZi (named pLacZ-3CArGM). cDNA cloning by the yeast one-hybrid system was performed as described previously using the MATCHMAKER One-Hybrid System (Clontech, Palo Alto, CA) (16). pLacZ-3CArGM and pHISi-3CArGM were integrated into the yeast (YM4271) genome. Next, the yeast was transformed with a human adult kidney cDNA library (Clontech), which contains a human kidney cDNA library cloned into pACT2 and produces the yeast GAL4 activation domain-cDNA fusion protein. Transformants were selected on uracil-, histidine-, and leucine-deficient plates that contained 20 mM 3-aminotriazole. Large colonies (His^+) were assayed for β-galactosidase activity by incubating at 30°C with a buffer that contained 0.8 mM 5-bromo-4-chloro-3-indolyl-β-D-galactopyranoside. Plasmids were isolated from blue colonies ($LacZ^+$), and their insert cDNA was analyzed by DNA sequencing.

Transfection Analysis of C/EBPδ

cDNA that contained the full coding region of human C/EBPδ was obtained by yeast one-hybrid analysis and inserted into the *Eco*RI site of pCAGGS (named pCAGGS-C/EBPδ). The 180-bp sequence of SMαA intron1 region from bp + 972, which contains an intronic CArG motif, or three tandem copies of the 20-bp intronic CArG motif (bp + 1093 to bp + 1112) were inserted into pSV0-CAT plasmid to construct reporter plasmids for transfection assay, designated as pSV-int180-CAT and pSV-3CArG-CAT, respectively. NIH-3T3 fibroblasts were seeded for transfection assay into 6-cm dishes at a density of 4×10^4 cells/cm^2. For each dish, 0.5 μg of reporter plasmid, 0 to 4 μg of expression plasmid, and 0.5 μg of luciferase reporter plasmid were transiently transfected with Lipofectamine Reagent (Life Technologies BRL). After 72 h, cells were harvested by scraping in lysis buffer. Promoter activities were evaluated by CAT and luciferase assays.

Preparation of C/EBPδ Protein and Electrophoretic Gel Mobility Shift Assay

Glutathione S-transferase (GST)-C/EBPδ was constructed in a pGEX 6P-1 vector (Amersham Pharmacia Biotech, Piscataway, NJ). GST-C/EBPδ was transformed into *Escherichia coli* BL21 and induced by 1 mM isopropyl-D-thiogalactopyranoside. Recombinant proteins were purified using glutathione-Sepharose 4B gels. The probe for the CArG motif (CArG #0) consists of 5'-GTTTTACCTAATT-AGGAAATGCTT and 5'-AAGCATTTCCTAATTAGGTAAAAC annealed to each other. The probe for C/EBPδ consensus consists of 5'-TGCAGATTGCGCAATCTGCA annealed to itself. Both oligonucleotides were 5'-end-labeled by T4 polynucleotide kinase with [γ-^{32}P]ATP (Amersham Biosciences, Tokyo, Japan). Binding reactions were performed in a 20-μl reaction mixture that contained binding buffer, 0.1 μg of C/EBPδ protein, 1 μg of poly-dIdC, and probe. Samples were incubated at room temperature for 30 min and fractionated on 5% polyacrylamide native gels in 0.5× Tris-borate EDTA buffer. After drying, gels were analyzed using the BAS system (Fujifilm, Tokyo, Japan). Competition assays were performed by adding nonlabeled C/EBP consensus probe or nonlabeled CArG #0 probe.

Renal Disease Models of Rat and Mouse

Acute mesangioproliferative glomerulonephritis was produced in rats by a single injection of anti-Thy1 monoclonal antibody (OX-7). On day 0, anti-Thy1 antibody was injected into the tail vein of 6-wk-old male rats at a dose of 1.5 mg/kg body wt (17). On day 7, kidneys were perfused with ice-cold PBS and removed. Habu-venom glomerulonephritis (HVGN), a murine model for acute mesangioproliferative glomerulonephritis, was induced in 6- to 8-wk-old male C/EBPδ(−/−) and C/EBPδ(+/+) mice. For inducing HVGN, heminephrectomized mice received an injection of lyophilized venom from Habu snake *Trimeresurus flavoviridis* (Wako, Osaka, Japan) dissolved in saline at 1.5 mg/kg body wt, and their urine was collected twice a week. Eight and 14 d after disease induction, mice were killed, and their kidneys and blood samples were collected (13).

Glomeruli Isolation, RNA Extraction, and Reverse Transcription–PCR

Total RNA of cultured cells and glomeruli were isolated using TRIzol reagent (Life Technologies BRL). Glomeruli were isolated from kidney by a differential sieving method (15). Kidneys were removed from killed animals, and renal cortices were dissected from the kidney with a scalpel, then minced and passed through stainless steel mesh of different pore sizes (120, 75, and 53 μm). Glomeruli were retained on the last mesh with a purity of >95%, as indicated by microscopic evaluation (the remaining few percent consisted of tubular fragments). cDNA was prepared from 1 μg of each RNA sample, using MuLV reverse transcriptase (Applied Biosystems, Foster City, CA), random hexamers, RNase inhibitor, and dNTP mixture in a final volume 20 μl. Semiquantitative PCR was performed with 1 μl of template cDNA, PCR primers (10 pmol each), and AmpliTaq DNA Polymerase (Applied Biosystems) in a final volume of 20 μl. PCR

products were analyzed by 2% agarose gel electrophoresis and stained with ethidium bromide. Primers used were murine SMαA 5'-ATCGTCCACCGCAAATGC (forward) and 5'-AAGGAACTGGAGGCGCTG (reverse); glyceraldehyde-3-phosphate dehydrogenase 5'-AGTATGACTCCACTCACGGCAA (forward) and 5'-TCTCGCTCCTGGAAGATGGT (reverse); C/EBPδ 5'-GCAGACAGTGGTGAGCTTGG (forward) and 5'-AAGCATGCGCAGTCTCTTCC (reverse); and monocyte chemoattractant protein-1 (MCP-1) 5'-AGCCAACTCTCACTGAAGCC (forward) and 5'-CATTCAAAGGTGCTGAAGACC (reverse).

Immunohistochemistry

Mouse monoclonal anti-SMαA (1A4; peroxidase conjugate DAKO, Glostrup, Denmark) and rabbit polyclonal anti-C/EBPδ antibody (Santa Cruz Biotechnology, Santa Cruz, CA) were used for immunohistochemical detection of SMαA and C/EBPδ. Paraffin-embedded sections (2-μm thickness) obtained from tissues fixed in 4% paraformaldehyde were blocked and incubated overnight with primary antibodies at 4°C. Sections for C/EBPδ immunostaining were incubated with the second biotinylated goat anti-rabbit antibody at 1:150 (Vector ABC Kit; Vector Laboratories, Burlingame, CA) for 1 h at room temperature, then incubated in an avidin-biotinylated horseradish peroxidase complex (Vector) for 40 min at room temperature. Peroxidase activity was visualized with *p*-dimethyl aminobenzaldehyde (DAB). For evaluating the quantitative level of SMαA expression in glomeruli, the outline of the glomeruli was encircled on the computer display, and the SMαA-positive (DAB-positive) area was determined by color density. The SMαA-positive area percentage (DAB-positive area/encircled area) was calculated from 30 glomeruli in each group using MacSCOPE software (Mitani-Corp, Fukui, Japan).

Results

Cloning of Intronic CArG Motif Binding Factor

To identify factors that bind to the CArG motif in intron 1 of SMαA gene, we used a yeast one-hybrid screening system. Approximately 5×10^6 human kidney cDNA clones were screened, and 38 double-positive clones were obtained. After sequence analysis, 20 of the 38 clones represented the same binding factor, identified as C/EBPδ (Figure 1), containing the sequence of the DNA-binding domain. These results indicate that C/EBPδ is a candidate for the intronic CArG motif binding.

Confirmation of Specific Binding of C/EBPδ to Intronic CArG Motif

As we assumed that the intronic CArG motif overlaps with a sequence compatible with the consensus sequence for the C/EBP family (T[T/G]NNGNAA[T/G]) (18) as shown by the underline in Figure 2a, and to exclude the possibility that the point-mutated CArG motif used in yeast one-hybrid cloning might have affected the binding reactivity, we performed electromobility shift assay to confirm binding of C/EBPδ to the original intronic CArG motif in SMαA. C/EBPδ protein produced in *E. coli* showed binding not only to C/EBP consensus sequence (Figure 2b) but also to the intronic CArG sequence (Figure 2c). Complex formation was inhibited after preincubation with unlabeled C/EBP consensus sequence and also, although less competitive, with unlabeled intronic CArG sequence. These results demonstrate the sequence-specific binding of C/EBPδ to the intronic CArG sequence.

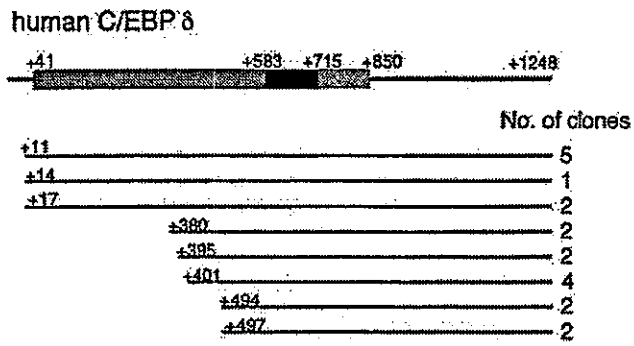

Figure 1. Domain structure of human CCAAT/enhancer-binding protein δ (C/EBPδ) gene (GenBank accession no. NM_005195) (top) and cDNA clones obtained from yeast one-hybrid analysis (bottom). Each cloned cDNA was produced from the 3'-polyA region. In the coding region, shown by a thick line, gray box (bp + 41 to bp + 583), filled box (bp + 583 to bp + 715), and hatched box (bp + 715 to bp + 850) represent transcription activating domain, DNA-binding domain, and leucine-zipper domain, respectively. Numbers of obtained clones are indicated on the right of each bar.

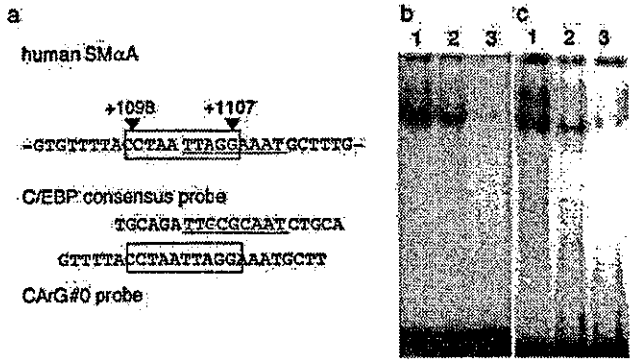

Figure 2. Electromobility shift assay (EMSA) detecting complex formation of *in vitro* translated C/EBPδ protein and probes. (a) The intronic CArG motif (CArG#0) and its flanking sequence (top) and sequences of the probes used for EMSA (bottom). The boxed sequence (from bp + 1098 to bp + 1107) represents the CArG motif ($CC[A/T]_6GG$), and the underlined sequence represents the C/EBP consensus (T[T/G]NNGNAA[T/G]); N, any nucleotide. (b and c) EMSA of C/EBPδ protein with C/EBP consensus probe (b) or the CArG#0 probe (c). Lane 1 is without competitor DNA, and lanes 2 and 3 are incubated with nonlabeled CArG#0 (×200) and C/EBP consensus (×200) oligonucleotides, respectively.

Transcriptional Activation of Intronic CArG Motif by C/EBPδ

To investigate whether C/EBPδ affects SMαA gene expression, we tested the transcriptional activity of reporter plasmid (pSV-int180-CAT), which contains 180 bp of SMαA intron 1 including the CArG motif as enhancer and CAT gene as reporter, by co-transfecting to NIH-3T3 fibroblasts with

C/EBPδ expression vector (pCAGGS-C/EBPδ). CAT activity of pSV-int180-CAT vector was increased by the co-transfection of pCAGGS-C/EBPδ vector in a dose-dependent manner up to 0.5 μg/dish with a 220% increase (Figure 3a). NIH-3T3 fibroblasts do not express SMαA in the basal condition, and this result suggests that C/EBPδ itself has positive activity through SMαA intron 1. Next, pSV-3CArG-CAT, which contains three copies of the 20-bp intronic CArG motif, was co-transfected with pCAGGS-C/EBPδ vector into NIH3T3 fibroblasts, showing a significant increase in CAT activity (180% with 0.5 μg/dish) compared with absence of pCAGGS-C/EBPδ (Figure 3b). As it has been reported that the sequence in intron 1 is essential for SMαA gene transcriptional activation (12,13), these results demonstrate involvement of C/EBPδ in transcriptional activation of SMαA gene *via* the intronic CArG motif.

Upregulation of SMαA and C/EBPδ in Rat Anti-Thy1 Glomerulonephritis

To investigate the *in vivo* relevance of C/EBPδ expression to myofibroblasts, we examined expression of C/EBPδ and SMαA in rat experimental mesangioproliferative glomerulonephritis. Reverse transcriptase–PCR analysis of SMαA and C/EBPδ mRNA was performed in isolated glomeruli obtained from untreated and anti-Thy1 glomerulonephritis rats on day 7. Both SMαA and C/EBPδ mRNA were upregulated in anti-Thy1 glomerulonephritis (Figure 4a). In immunohistochemical examination with consecutive sections from untreated rats, staining of SMαA was observed only in smooth muscle of the arteriolar wall (Figure 4b), and positive staining of C/EBPδ was minute in both glomerulus and arteriolar wall (Figure 4d). In contrast, anti-Thy1 glomerulonephritis rat showed SMαA and C/EBPδ immunostaining in glomerulus with similar distribution (Figure 4, c and e).

SMαA Expression in Cultured Mesangial Cells from C/EBPδ(−/−) Mice

Cultured mesangial cells express substantial amounts of SMαA and are thought to mimic activated mesangial cells, namely myofibroblasts, found in diseased glomeruli (19). As C/EBPδ(−/−) mice have been produced before and reported to exhibit little phenotypic modulation under physiologic conditions (14), we investigated expression levels of SMαA in cultured mesangial cells from these knockout mice. Expression of SMαA mRNA in C/EBPδ(−/−) cells was lower than that in C/EBPδ(+/+) cells (Figure 5). Moreover, mRNA expression of MCP-1, which is considered an important chemokine in the progression of glomerulonephritis, was also reduced in C/EBPδ(−/−) mesangial cells (Figure 5). However, other proinflammatory cytokines, such as TGF-β1 and IL-1β, did not show a reduction in their mRNA levels, compared with C/EBPδ(+/+) cultured mesangial cells (data not shown).

Renal Disease Model in C/EBPδ(−/−) Mice

Mouse HVGN is a model for acute mesangioproliferative glomerulonephritis, which evokes acute mesangiolysis followed by mesangial cell proliferation with myofibroblastic transdifferentiation and matrix increment. Similar to rat anti-Thy1 glomerulonephritis, C/EBPδ expression was only slightly observed in normal glomeruli and increased in HVGN in C/EBPδ(+/+) mice but not at all in C/EBPδ(−/−) mice (Figure 6).

Mesangial SMαA expression in C/EBPδ(−/−) mice on day 8 was milder than in C/EBPδ(+/+) mice (Figure 7, c and d). Although mesangial expansion was observed to persist in HVGN on day 14, mesangial SMαA expression was diminished in both C/EBPδ(+/+) and C/EBPδ(−/−) mice at that time (Figure 7, g and h), possibly suggesting that the disease was going into the recovery phase. The proportion of glomerular SMαA-positive area in C/EBPδ(−/−) mice was significantly less (11.0 ± 6.9 *versus* 18.2 ± 8.7%; mean ± SD) than in C/EBPδ(+/+) mice (Figure 7i). These data suggest involvement of C/EBPδ in mesangial transdifferentiation and SMαA expression in acute mesangioproliferative glomerulonephritis. Urinary protein excretion tended to be decreased along the time course of HVGN in C/EBPδ(−/−) mice *versus* C/EBPδ(+/+) mice. The urinary protein/creatinine ratios were 5.0 ± 2.9 *versus* 7.6 ± 1.6 on day 4 and 3.6 ± 0.8 *versus* 4.3 ± 0.7 on day 14 for C/EBPδ(−/−) mice *versus* C/EBPδ(+/+), respectively. The renal function was preserved in C/EBPδ(−/−)

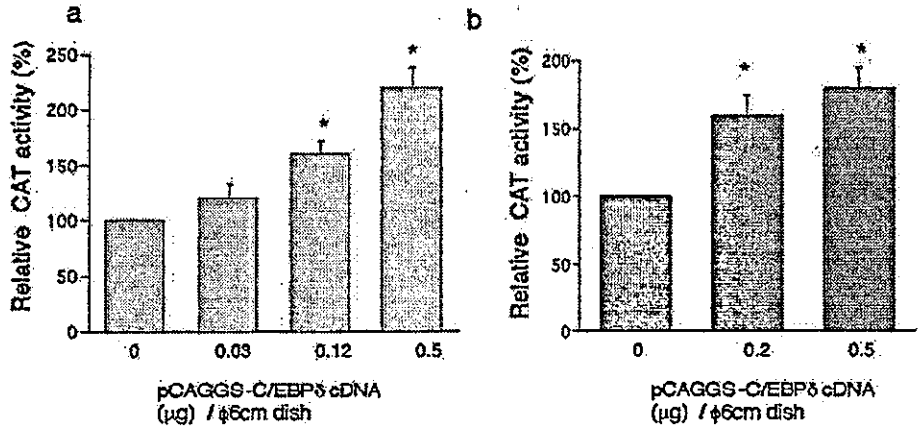

Figure 3. Co-transfection analysis of the interaction of C/EBPδ with sequence including CArG#0. pSV-int180-CAT (a) or pSV-3CArG-CAT (b) was co-transfected with pCAGGS-C/EBPδ into NIH-3T3 fibroblasts. Data are obtained from five repetitive experiments. CAT activity was corrected by luciferase activity in each transfection. Relative CAT activity was determined as the ratio of activity when co-transfected with pCAGGS only. Values are expressed as mean ± SD; $^*P < 0.01$.

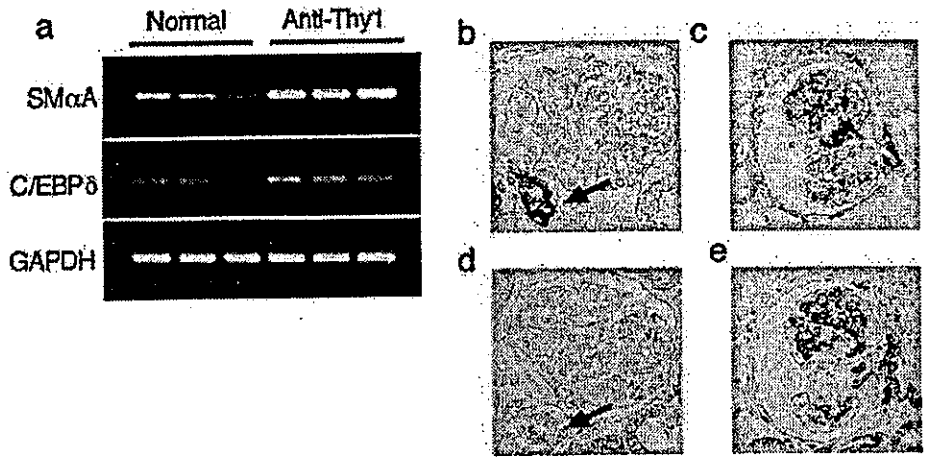

Figure 4. Assessment of smooth muscle α-actin (SMαA) and C/EBPδ expression in anti-Thy1 glomerulonephritis. (a) Reverse transcriptase–PCR (RT-PCR) detection of SMαA (top), C/EBPδ (middle), and glyceraldehyde-3-phosphate dehydrogenase (GAPDH; bottom) mRNA in isolated glomeruli from untreated rats (left three lanes) and from anti-Thy1 glomerulonephritis rats on day 7 (right three lanes). Each lane represents an individual rat. (b through e) Immunostaining for SMαA (b and c) and C/EBPδ (d and e) in consecutive sections of the same glomerulus from untreated rat (b and d) and anti-Thy1 glomerulonephritis rat (c and e). Arrows in b and d indicate arteriolar walls. Magnification, ×400.

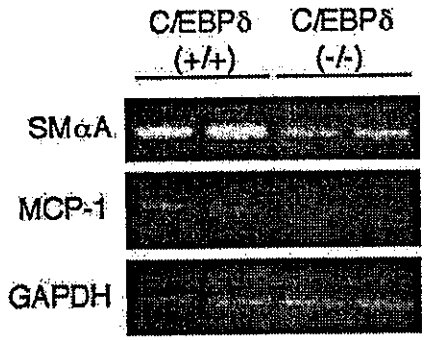

Figure 5. mRNA expression of SMαA (top) and monocyte chemoattractant protein-1 (MCP-1; middle) in mesangial cells in culture assessed by RT-PCR. mRNA extracted from C/EBPδ(+/+) mesangial cells is indicated in the left two lanes, and mRNA from C/EBPδ(−/−) mesangial cells is indicated in the right two lanes.

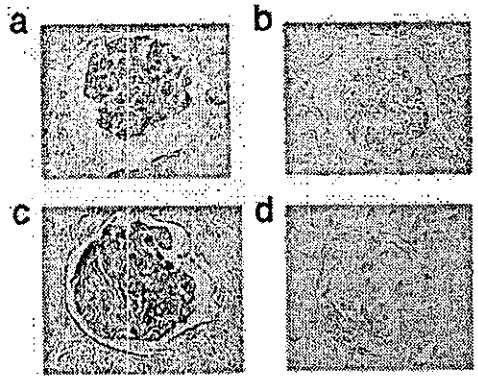

Figure 6. Immunohistochemistry of C/EBPδ in the glomerulus of C/EBPδ (+/+) (a and c) and C/EBPδ (−/−) (b and d) mice. (a and b) Normal condition. (b and d) Habu-venom glomerulonephritis (HVGN) on day 8. Magnification, ×400.

mice. Plasma urea nitrogen was 39.3 ± 2.6 *versus* 56.9 ± 16.6 and plasma creatinine 0.15 ± 0.02 *versus* 0.20 ± 0.04 on day 14 (mg/dl, mean ± SD; $P < 0.05$) for C/EBPδ(−/−) mice *versus* C/EBPδ(+/+), respectively.

Discussion

We have been investigating the pathophysiologic significance, nature, and molecular mechanism of phenotypic change of renal cells to myofibroblasts in the process of progressive renal diseases (4,5,13). We hypothesized that the molecular mechanisms underlying the induction of SMαA in myofibroblasts are closely related to the molecular pathophysiology of progressive renal disease leading to renal fibrosis. The intronic CArG motif from the SMαA gene is essential for *in vivo* transcriptional activation of the SMαA gene in both smooth muscle cells (12) and renal myofibroblasts (13). Interaction of the CArG motif and SRF is a candidate mechanism for transcriptional activation of the SMαA gene (20,21). However, SRF is a ubiquitous factor, and the CArG motifs are present in a wide variety of genes. We identified C/EBPδ as the major candidate transcription factor for transactivating the SMαA gene in myofibroblasts through its intronic CArG sequence. We also found that C/EBPδ can bind directly to DNA in contrast to myocardin, a key co-factor of SRF (22) for smooth muscle differentiation co-activating SMαA and other smooth muscle gene expression in smooth muscle cells (23,24). We observed that there was no expression of myocardin mRNA in both normal and diseased kidney or cultured mesangial cells (unpublished observation), so its involvement in myofibroblast transdifferentiation is unlikely. It is, however, still unknown whether C/EBPδ can cooperate with SRF and/or other transcription factors.

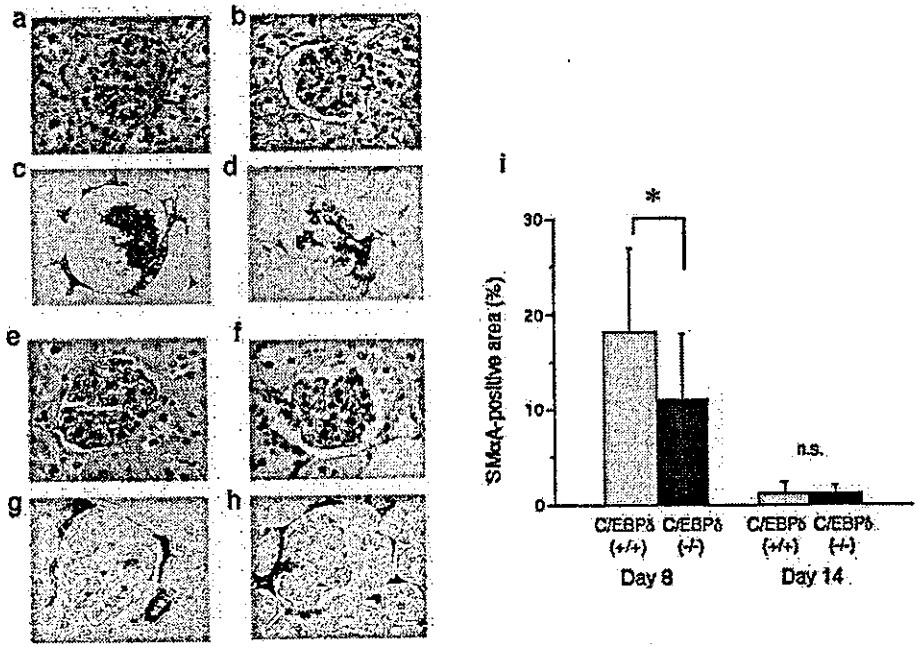

Figure 7. Histologic assessment by periodic acid-Schiff staining (a, b, e, and f) and immunohistochemistry of SMαA (c, d, g, and h) in HVGN on day 8 (a through d) and day 14 (e and f). (a, c, e, and g) C/EBPδ(+/+) mice. (b, d, f, h) C/EBPδ(−/−) mice. (i) Quantitative evaluation of glomerular SMαA expression. Values are mean ± SD, calculated from 30 glomeruli in each group; $*P <$ 0.001. Magnification, ×400.

C/EBPδ belongs to the C/EBP family, which contains a leucine zipper domain that mediates dimerization with the same or other C/EBP isoforms and interaction with the target sequence. In the present study, we found that C/EBPδ can bind to the C/EBP family consensus sequence, which coincides with the intronic CArG sequence and can stimulate promoter activity of the SMαA gene through it (Figures 2 and 3). In addition, as shown in Figure 4, C/EBPδ and SMαA proteins were upregulated and distributed similarly in the mesangial area in experimental glomerulonephritis. In contrast, in smooth muscle cells of the arteriolar wall, SMαA immunostaining is densely positive but C/EBPδ staining is not (Figure 4, b and d). This observation indicates that, in normal smooth muscle cells, C/EBPδ is not greatly involved in the expression of SMαA. This result is the first demonstration of upregulation of C/EBPδ in myofibroblasts *in vivo* in experimental glomerulonephritis and strongly suggests a pivotal role for C/EBPδ in the positive regulation of SMαA in glomerular myofibroblasts.

We found that *in vitro* cultured mesangial cells isolated from C/EBPδ(−/−) mice express much less SMαA compared with those from C/EBPδ(+/+) mice (Figure 5), supporting the *in vivo* observation of possible involvement of C/EBPδ in gene regulation of SMαA in glomerular myofibroblasts. Moreover, the mesangioproliferative glomerulonephritis model (HVGN) in C/EBPδ(−/−) mice showed decreased SMαA expression in the glomeruli *in vivo* (Figure 7).

Myofibroblasts are also known to play pivotal roles in the progression of tubulointerstitial fibrosis. There arose a possibility that C/EBPδ might be involved with myofibroblasts not only in glomerular mesangial lesions but also in tubulointerstitial lesions; thus, we investigated another renal disease model. Unilateral ureteral obstruction (UUO) is a model of tubulointerstitial fibrosis, in which we previously reported that the emergence of myofibroblast was closely related to the degree of fibrosis (25,26). We analyzed UUO in C/EBPδ(−/−) mice and found that SMαA mRNA upregulation in whole kidneys of UUO (on day 7) was significantly attenuated in C/EBPδ(−/−) mice compared with C/EBPδ(+/+) mice (data not shown). In addition to results from the HVGN model, these results suggest that C/EBPδ is engaged in the process of transdifferentiation not only in mesangial cells but also in renal interstitial fibroblasts and might play a role in exacerbation of progressive renal diseases.

C/EBPδ is expressed in liver, lung, adipose tissue, and intestine under physiologic conditions and is strongly upregulated at the transcriptional level by inflammatory stimuli, such as turpentine oil, bacterial LPS, and cytokines such as IL-6 and TNF-α (27,28). C/EBPδ(−/−) mouse shows only a mild phenotype of slightly disturbed lipid storage under physiologic conditions (14). These findings indicate that C/EBPδ is not essential for development and/or maintenance of these tissues, perhaps because of the redundant function of other C/EBP family proteins. Some investigators have reported a role for C/EBPδ in pathologic states. For example, C/EBPδ enhances PDGF-α receptor expression in vascular smooth muscle cells, and its contribution to atherosclerosis is suggested (29). The present report is the first to show the relationship between C/EBPδ and kidney disease, suggesting the possibility of attenuation of the disease by suppressing C/EBPδ activity. In the pathologic state of other organs to which SMαA-expressing myofibroblasts contribute, such as liver cirrhosis, chronic pancreatitis, and pulmonary fibrosis, C/EBPδ may also play an important role.

Myofibroblasts are thought to be a source of extracellular matrix deposition in sclerosing tissues. C/EBP binding sites have been identified in the promoters of several genes that

modulate extracellular matrix expansion, such as type I collagen or tissue inhibitor of metalloproteinases (30,31). It is interesting that C/EBP were reported to regulate type I collagen transcription in hepatic stellate cells through a hydrogen peroxide–dependent pathway (32,33). The binding motifs for C/EBP are now known to be present in various genes that encode most inflammation-inducible molecules, such as IL-1β, MCP-1 (34), granulocyte macrophage colony-stimulating factor receptor gene (35), PDGF receptor (29,36), and intercellular adhesion molecule 1 (37). In the present study, MCP-1 mRNA expression was clearly decreased in C/EBPδ(−/−) mesangial cells in culture, but we could see no obvious difference for other cytokines, including TGF-β1, a key mediator of myofibroblast transdifferentiation (38,39). This may be due to the degree of replacement of other transcription factor(s), perhaps including C/EBPβ, and for MCP-1 transcription, C/EBPδ may have a major contribution.

In the present study, C/EBPδ(−/−) mice showed less SMαA expression in HVGN on day 7, and consequent renal function was relatively less deteriorated. These results suggest that suppressing excessive myofibroblast transdifferentiation could be a therapeutic measure for glomerulonephritis. A recent report pointed out that myofibroblasts are necessary in the repair process of kidney tissue injury (40); however, the present results show amelioration of renal disease by partial inhibition of myofibroblast transdifferentiation in the absence of C/EBPδ. Certainly, from the present data, we cannot conclude whether it is beneficial to block the transdifferentiation completely, and further investigation is planned.

In conclusion, we have determined that the intronic CArG motif in SMαA gene is a binding locus of transcriptional activator C/EBPδ. C/EBPδ was upregulated in rat and mouse experimental glomerulonephritis, and its expression mirrored SMαA induction. SMαA expression was lower in cultured mesangial cells and renal disease models in C/EBPδ(−/−) mice compared with C/EBPδ(+/+) mice. Furthermore, the degree of renal function loss was attenuated in C/EBPδ(−/−) mice. Our results demonstrate the involvement of C/EBPδ in transcriptional activation of the SMαA gene in myofibroblasts and in renal diseases. Further analysis of C/EBPδ-dependent gene regulation in myofibroblasts is likely to give us new insights into molecular pathophysiology of progressive renal disease and helps in establishing new therapeutic approaches to myofibroblast-related disease.

Acknowledgments

This work has been supported by a grant-in-aid for scientific research from the Ministry of Education, Culture, Sports, Science and Technology, Japan (T.M.), and by a grant from Takeda Science Foundation (T.M.).

We are grateful to Dr. Wataru Nishida (Department of Neuroscience, Osaka University) for help in preparing GST-C/EBPδ fusion protein.

References

1. Brenner DA, Waterboer T, Sung Kyu C, Lindquist JN, Stefanovic B, Burchardt E, Yamauchi M, Gillan A, Rippe RA: New aspects of hepatic fibrosis. *J Hepatol* 32[Suppl 1]: 32–38, 2000
2. Badid C, Mounier N, Costa AM, Desmouliere A: Role of myofibroblasts during normal tissue repair and excessive scarring: Interest of their assessment in nephropathies. *Histol Histopathol* 15: 269–280, 2000
3. Powell DW, Mifflin RC, Valentich JD, Crowe SE, Saada JI, West AB: Myofibroblasts. I. Paracrine cells important in health and disease. *Am J Physiol* 277: C1–C9, 1999
4. Ando Y, Moriyama T, Miyazaki M, Akagi Y, Kawada N, Isaka Y, Izumi M, Yokoyama K, Yamauchi A, Horio M, Ando A, Ueda N, Sobue K, Imai E, Hori M: Enhanced glomerular expression of caldesmon in IgA nephropathy and its suppression by glucocorticoid-heparin therapy. *Nephrol Dial Transplant* 13: 1168–1175, 1998
5. Ando Y, Moriyama T, Oka K, Takatsuji K, Miyazaki M, Akagi Y, Kawada N, Isaka Y, Izumi M, Yokoyama K, Yamauchi A, Horio M, Ando A, Ueda N, Sobue K, Imai E, Hori M: Enhanced interstitial expression of caldesmon in IgA nephropathy and its suppression by glucocorticoid-heparin therapy. *Nephrol Dial Transplant* 14: 1408–1417, 1999
6. Goumenos DS, Brown CB, Shortland J, el Nahas AM: Myofibroblasts, predictors of progression of mesangial IgA nephropathy? *Nephrol Dial Transplant* 9: 1418–1425, 1994
7. Goumenos D, Tsomi K, Iatrou C, Oldroyd S, Sungur A, Papaioannides D, Moustakas G, Ziroyannis P, Mountokalakis T, El Nahas AM: Myofibroblasts and the progression of crescentic glomerulonephritis. *Nephrol Dial Transplant* 13: 1652–1661, 1998
8. MacPherson BR, Leslie KO, Lizaso KV, Schwarz JE: Contractile cells of the kidney in primary glomerular disorders: An immunohistochemical study using an anti-alpha-smooth muscle actin monoclonal antibody. *Hum Pathol* 24: 710–716, 1993
9. Groma V, Marcussen N, Olsen S: A quantitative immunohistochemical study of the expression of mesangial alpha-smooth muscle actin and the proliferation marker Ki-67 in glomerulonephritis in man. *Virchows Arch* 431: 345–350, 1997
10. Makino H, Kashihara N, Sugiyama H, Kanao K, Sekikawa T, Okamoto K, Maeshima Y, Ota Z, Nagai R: Phenotypic modulation of the mesangium reflected by contractile proteins in diabetes. *Diabetes* 45: 488–495, 1996
11. Pilmore HL, Painter DM, Bishop GA, McCaughan GW, Eris JM: Early up-regulation of macrophages and myofibroblasts: A new marker for development of chronic renal allograft rejection. *Transplantation* 69: 2658–2662, 2000
12. Mack CP, Owens GK: Regulation of smooth muscle alpha-actin expression in vivo is dependent on CArG elements within the 5' and first intron promoter regions. *Circ Res* 84: 852–861, 1999
13. Kawada N, Moriyama T, Ando A, Koyama T, Hori M, Miwa T, Imai E: Role of intron 1 in smooth muscle alpha-actin transcriptional regulation in activated mesangial cells in vivo. *Kidney Int* 55: 2338–2348, 1999
14. Tanaka T, Yoshida N, Kishimoto T, Akira S: Defective adipocyte differentiation in mice lacking the C/EBPβ and/or C/EBPΔ gene. *EMBO J* 16: 7432–7443, 1997
15. Moriyama T, Fujibayashi M, Fujiwara Y, Kaneko T, Xia C, Imai E, Kamada T, Ando A, Ueda N: Angiotensin II stimulates interleukin-6 release from cultured mouse mesangial cells. *J Am Soc Nephrol* 6: 95–101, 1995
16. Ishida H, Ueda K, Ohkawa K, Kanazawa Y, Hosui A, Nakanishi F, Mita E, Kasahara A, Sasaki Y, Hori M, Hayashi N: Identification of multiple transcription factors, HLF, FTF, and E4BP4, controlling hepatitis B virus enhancer II. *J Virol* 74: 1241–1251, 2000

17. Yamamoto T, Wilson CB: Quantitative and qualitative studies of antibody-induced mesangial cell damage in the rat. *Kidney Int* 32: 514–525, 1987
18. Akira S, Isshiki H, Sugita T, Tanabe O, Kinoshita S, Nishio Y, Nakajima T, Hirano T, Kishimoto T: A nuclear factor for IL-6 expression (NF-IL6) is a member of a C/EBP family. *EMBO J* 9: 1897–1906, 1990
19. Elger M, Drenckhahn D, Nobiling R, Mundel P, Kriz W: Cultured rat mesangial cells contain smooth muscle alpha-actin not found in vivo. *Am J Pathol* 142: 497–509, 1993
20. Simonson MS, Walsh K, Kumar CC, Bushel P, Herman WH: Two proximal CArG elements regulate SM alpha-actin promoter, a genetic marker of activated phenotype of mesangial cells. *Am J Physiol* 268: F760–F769, 1995
21. Treisman R, Ammerer G: The SRF and MCM1 transcription factors. *Curr Opin Genet Dev* 2: 221–226, 1992
22. Wang D, Chang PS, Wang Z, Sutherland L, Richardson JA, Small E, Krieg PA, Olson EN: Activation of cardiac gene expression by myocardin, a transcriptional cofactor for serum response factor. *Cell* 105: 851–862, 2001
23. Yoshida T, Sinha S, Dandre F, Wamhoff BR, Hoofnagle MH, Kremer BE, Wang DZ, Olson EN, Owens GK: Myocardin is a key regulator of CArG-dependent transcription of multiple smooth muscle marker genes. *Circ Res* 92: 856–864, 2003
24. Wang Z, Wang DZ, Pipes GC, Olson EN: Myocardin is a master regulator of smooth muscle gene expression. *Proc Natl Acad Sci U S A* 100: 7129–7134, 2003
25. Kawada N, Moriyama T, Ando A, Fukunaga M, Miyata T, Kurokawa K, Imai E, Hori M: Increased oxidative stress in mouse kidneys with unilateral ureteral obstruction. *Kidney Int* 56: 1004–1013, 1999
26. Nagatoya K, Moriyama T, Kawada N, Takeji M, Oseto S, Murozono T, Ando A, Imai E, Hori M: Y-27632 prevents tubulointerstitial fibrosis in mouse kidneys with unilateral ureteral obstruction. *Kidney Int* 61: 1684–1695, 2002
27. Alam T, An MR, Papaconstantinou J: Differential expression of three C/EBP isoforms in multiple tissues during the acute phase response. *J Biol Chem* 267: 5021–5024, 1992
28. Akira S, Kishimoto T: NF-IL6 and NF-kappa B in cytokine gene regulation. *Adv Immunol* 65: 1–46, 1997
29. Yang ZH, Kitami Y, Takata Y, Okura T, Hiwada K: Targeted overexpression of CCAAT/enhancer-binding protein-delta evokes enhanced gene transcription of platelet-derived growth factor alpha-receptor in vascular smooth muscle cells. *Circ Res* 89: 503–508, 2001
30. Diehl AM: Roles of CCAAT/enhancer-binding proteins in regulation of liver regenerative growth. *J Biol Chem* 273: 30843–30846, 1998
31. Ponton A, Coulombe B, Steyaert A, Williams BR, Skup D: Basal expression of the gene (TIMP) encoding the murine tissue inhibitor of metalloproteinases is mediated through AP1- and CCAAT-binding factors. *Gene* 116: 187–194, 1992
32. Garcia-Trevijano ER, Iraburu MJ, Fontana L, Dominguez-Rosales JA, Auster A, Covarrubias-Pinedo A, Rojkind M: Transforming growth factor β1 induces the expression of α1(I) procollagen mRNA by a hydrogen peroxide-C/EBPβ-dependent mechanism in rat hepatic stellate cells. *Hepatology* 29: 960–970, 1999
33. Greenwel P, Dominguez-Rosales JA, Mavi G, Rivas-Estilla AM, Rojkind M: Hydrogen peroxide: A link between acetaldehyde-elicited alpha1(I) collagen gene up-regulation and oxidative stress in mouse hepatic stellate cells. *Hepatology* 31: 109–116, 2000
34. Hu HM, Baer M, Williams SC, Johnson PF, Schwartz RC: Redundancy of C/EBP alpha, -beta, and -delta in supporting the lipopolysaccharide-induced transcription of IL-6 and monocyte chemoattractant protein-1. *J Immunol* 160: 2334–2342, 1998
35. van Dijk TB, Baltus B, Raaijmakers JA, Lammers JW, Koenderman L, de Groot RP: A composite C/EBP binding site is essential for the activity of the promoter of the IL-3/IL-5/granulocyte-macrophage colony-stimulating factor receptor beta c gene. *J Immunol* 163: 2674–2680, 1999
36. Kitami Y, Fukuoka T, Hiwada K, Inagami T: A high level of CCAAT-enhancer binding protein-delta expression is a major determinant for markedly elevated differential gene expression of the platelet-derived growth factor-alpha receptor in vascular smooth muscle cells of genetically hypertensive rats. *Circ Res* 84: 64–73, 1999
37. Hou J, Baichwal V, Cao Z: Regulatory elements and transcription factors controlling basal and cytokine-induced expression of the gene encoding intercellular adhesion molecule 1. *Proc Natl Acad Sci U S A* 91: 11641–11645, 1994
38. Desmouliere A, Geinoz A, Gabbiani F, Gabbiani G: Transforming growth factor-beta 1 induces alpha-smooth muscle actin expression in granulation tissue myofibroblasts and in quiescent and growing cultured fibroblasts. *J Cell Biol* 122: 103–111, 1993
39. Roberts AB, Sporn MB, Assoian RK, Smith JM, Roche NS, Wakefield LM, Heine UI, Liotta LA, Falanga V, Kehrl JH, *et al.*: Transforming growth factor type beta: Rapid induction of fibrosis and angiogenesis in vivo and stimulation of collagen formation in vitro. *Proc Natl Acad Sci U S A* 83: 4167–4171, 1986
40. Sun DF, Fujigaki Y, Fujimoto T, Goto T, Yonemura K, Hishida A: Mycophenolate mofetil inhibits regenerative repair in uranyl acetate-induced acute renal failure by reduced interstitial cellular response. *Am J Pathol* 161: 217–227, 2002